

Date of publication xxxx 00, 0000, date of current version xxxx 00, 0000.9

Digital Object Identifier

Orbital Angular Momentum for Wireless Communications: Key Performance Indicators and Performance Comparison

ZIHAO WANG¹, MOHAMMED EL-HAJJAR, (Senior Member, IEEE,)¹, and LIE-LIANG YANG, (Fellow, IEEE)¹

¹School of Electronics and Computer Science, University of Southampton, Southampton SO17 1BJ, United Kingdom (email:{zw3e22,meh,lly}@ecs.soton.ac.uk). Corresponding author: Lie-liang Yang (e-mail: lly@ecs.soton.ac.uk).

The authors would like to acknowledge the financial support of the Engineering and Physical Sciences Research Council (EPSRC) projects under grants EP/X01228X/1, EP/X04047X/1 and EP/Y037243/1, as well as the Future Telecoms Research Hub, Platform for Driving Ultimate Connectivity (TITAN), sponsored by the Department of Science Innovation and Technology (DSIT).

ABSTRACT Orbital angular momentum (OAM) is an intrinsic property of electromagnetic (EM) waves that has opened new possibilities for enhancing the capacity of wireless communications. Consequently, it has garnered significant attention in recent years. For wireless communications, antenna arrays are the most effective and widely studied approaches for OAM-wave generation. Various types of antenna arrays have been explored in research and development; however, a comprehensive comparison of these arrays remains lacking. This paper addresses this gap by first reviewing the various types of phased arrays that have been considered for OAM generation in the literature. Subsequently, it addresses the key performance indicators (KPIs) of the antenna arrays for OAM-wave generation. These KPIs include directivity, the largest producible OAM-mode (LPM), OAM-mode multiplexing capability, divergence angle, and mode purity. Based on the KPIs, a comparative analysis is conducted across several types of antenna arrays, including uniform square arrays (USA), uniform circular arrays (UCA), three-dimensional (3D) helical circular arrays (HCA), 3D helical circular sub-arrays (HCSA), and concentric UCAs (CUCA), under various settings. The study highlights the advantages and limitations of each antenna array type and examines how different parameters influence their performance.

INDEX TERMS Wireless communications, orbital angular momentum (OAM), antenna array, phased array, key performance indicators, directivity, OAM-mode, divergence angle, purity, 6G communications.

I. INTRODUCTION

In the research and development of wireless communications, about every ten years, a new generation of wireless technologies has emerged since 1980. The designs of the first and second-generation (1G and 2G) wireless systems were mainly focused on symmetric traffic between uplink (UL) and downlink (DL) to support voice communications [1]. The third and, especially, the fourth-generation (3G and 4G) wireless systems were mainly focused on DL, to provide asymmetric UL/DL traffic resulting from the internet-based services [1]. From 1G to 4G, wireless systems have been centralized to support services around human beings. By contrast, since the fifth-generation (5G) released in 2020, wireless services have been expected to be supported in all possible dimensions, from classic mobile phones, tablets, to the various types of sensors, from voice transmission, internet, to industrial con-

trol commanding, from deep sea, indoor/outdoor, to space, from static or low-mobility environments, to median-mobility vehicular networks, to high-mobility high-speed trains or even flights, etc. [2]. Supporting such wireless services of multi-dimensional has been becoming possible, because the 5G techniques are capable of empowering wireless transmissions with extremely high data rates, ultra-reliable low latency, and massive connectivity [1, 2].

However, the techniques relying on the conventional resources in frequency, time and space domains have been actively researched and developed for many decades. It is becoming increasingly challenging to attain the capacity expected for supporting the future generations of wireless services [3]. According to ITU [4], global mobile traffic was about 7.5 exabyte (EB) per month in 2010 but is expected to increase more than 6,000 times in 2030, at the start of



the sixth-generation (6G) era [5]. To meet the challenges, researchers and industries throughout the world have been debating for the crucial technologies, perspectives, and service demands. Although the standards for 6G are not yet clear, it is commonly anticipated that 6G will support many new types of services and significantly enhanced services, demanding, such as, ultra-high data rates, ultra-reliable and ultra-low latency, ultra-massive connectivity, ultra-high precision, etc. [1,5].

Due to the above-mentioned, new resources have been introduced and researched for 6G wireless communications. Among them, the orbital angular momentum (OAM) allowed to embed with radio waves has emerged as one of the prominent candidates, and has undergone extensive investigation for applications in wireless communications in recent years [6]. Historically, Allen et al. in 1992 [7] discovered that light can carry OAM, which is defined by a topological charge known as mode number, commonly represented by a variable l in the literature. Here, l can be an infinite integer, indicating the number of 2π phase alternates around the crosssection of the beam's propagation direction over one wavelength of the propagation distance. However, the research on OAM has been restricted to optical field for a long time, until about fifteen years later when OAM was initially applied and numerically simulated in low radio frequency (RF) bands [8]. The feasibility of OAM for applications in wireless communications was experimentally verified in 2012 [9], which reignited the research interest, leading to numerous followed studies in wireless communications communities. The studies have considered various aspects, including OAMbeam generation [10–12], achievable spectrum efficiency and capacity [13-16], design and optimization of antenna arrays [17, 18], and purity analysis and performance [19–22].

The advantages of OAM lie in its property that the OAMwaves of different modes are orthogonal to each other [23, 24], which provides new degrees-of-freedom for wireless signalling design. Based on this property, multiple OAM-modes can be multiplexed and transmitted on a wave of identical frequency, thus, allowing to increase the throughput without increasing the bandwidth, yielding increased spectralefficiency [6]. This technique is referred to as OAM-mode division multiplexing (OAM-MDM). OAM-MDM can be added to many existing communication schemes [25, 26], including orthogonal frequency division multiplexing (OFDM) [27–29], frequency hopping [30], code division multiple access (CDMA) [31], non-orthogonal multiple access (NOMA) [32], and various index modulation (IM) schemes [33]. As a results, the capacity of the corresponding wireless systems can be improved without relying on extra resources from the conventional space, time and frequency domains.

Furthermore, OAM may be integrated with some 6G technologies, including Terahertz (THz), reconfigurable intelligent surface (RIS), security, holographic multiple-input multiple-output (MIMO), and internet of everything (IoE) [34–39]. To be more specific, first, OAM can provide additional dimensional resources for the design of THz sys-

tems [35, 36]. On the other side, THz signaling may also enhance the performance of QAM systems. According to [36], using a higher carrier frequency helps to reduce OAM's beam divergence. Second, OAM can be implemented for signal transmission between a base-station (BS) and its associated RISs to improve information transmission between them [40]. Since both BS and RISs are usually fixed apparatuses, the scenario is beneficial to the implementation of OAM. Third, for security application, the low-order OAMmodes may be configured for information transmission, while the high-order OAM-modes can be set to transmit artificial noise to mitigate the possibility of eavesdropping [37]. Furthermore, in [38], it was demonstrated that the active holographic MIMO metasurfaces is capable of exploiting the intrinsic orthogonality of OAM-beams to establish multiple parallel communication channels, thereby enhancing the spatial multiplexing capability and ultimately spectral-efficiency. Additionally, via the integration of OAM with a dynamic power-splitting scheme, a simultaneous wireless information and power transfer (SWIPT) system may flexibly divide received energy between information decoding and energy harvesting. This is crucial for powering the batteryless IoE devices in future 6G systems. Notably, as demonstrated in [39], when communicating over short-distance line-of-sight (LoS) channels, an OAM-assisted SWIPT system is capable of attaining a superior rate-energy trade-off, when compared with both the conventional single-input single-output (SISO) and MIMO systems.

Nevertheless, as the first step to applications, the generation of OAM-waves has garnered significant research attention. Accordingly, various methods have been explored, including those generating OAM-waves using spiral phase plate (SPP), parabolic antenna, phased array, dielectric resonator antenna (DRA), and metasurface [6, 41]. Among these methods, the antenna array method stands out as the main technique, owing to its feasibility for both indoor and outdoor applications, flexibility of beam steering, compact size, and reconfigurable capability [6]. Despite many advantages, the antenna array method still faces significant challenges that need to be addressed before practical applications. One of the main problems of OAM-waves is the beam divergence effect, which numerous researches have been endeavoured to alleviate [42–45]. For example, in [11] and [46], uniform circular arrays (UCAs) were designed for generating the OAMbeams carrying different modes to attain an equal divergence angle. In [44], a so-called transmit-array was designed to convey dual OAM-modes experiencing only small divergence effect. Another challenge with the antenna array method is the purity of OAM-beams generated, which reflects the quality of OAM-beams. Hence, research efforts have been made to maximize the OAM purity via optimizing the structures of the antenna arrays, as shown, for example, in [20, 22, 47].

However, the definitions of divergence angle and purity are different in different references, making the performance comparison across different schemes inconvenient. For example, in [20, 48–52], instead of absolute directivity, the relative

directivity of antenna arrays, with respect to the maximum of a particular array, is generally considered. This makes it difficult to compare the performance between different OAM-generating antenna arrays. Another issue is that UCA can be used to generate an OAM-wave conveying one specific mode, or alternatively, it can be configured to generate an OAM-wave simultaneously carrying multiple modes achieving mode multiplexing [53, 54]. Moreover, concentric uniform circular array (CUCA) is even more flexible than UCA, as each CUCA consists of several rings of sub-UCAs. Hence, these sub-UCAs can be treated as separate UCAs for generating OAM-beams of different modes, or treated

as one CUCA to jointly generate an OAM-beam carrying

multiple modes. Therefore, it is desirable to have an explicit

and comprehensive comparison of the UCAs and CUCAs

with different configurations. Additionally, the effect of array

parameters, such as the array structures, number of transmit

array elements, and number of receive array elements (sam-

pling points of phase profile), remains largely unexamined. To address the above-mentioned issues, under a unified framework, we provide a comprehensive comparison of the typical antenna arrays considered for OAM-wave generation, when antenna arrays are operated under different configurations. Our motivation is to analyze the OAM-generating arrays in terms of their merits and shortcomings, when practical applications under certain constraints are considered. Briefly, our contributions can be summarized as follows:

- Propose a unified framework for performance comparison between different OAM-generating antenna arrays, where five KPIs are introduced, encompassing directivity, beam divergence angle, OAM-mode purity, largest producible mode (LPM) and multiplexing capability.
- Analyze six types of antenna arrays, mainly investigated with OAM in the literature, including uniform linear array (ULA), uniform square array (USA), UCA, CUCA, three-dimensional (3D) helical circular array (HCA) and 3D helical circular sub-array (HCSA). Some of the other arrays less considered in the literatures are also briefly noted.
- Based on simulation results, USA, UCA, CUCA, 3D HCA and 3D HCSA are comprehensively compared against the KPIs, when they are configured to generate OAM-modes 1 to 4. For USA and UCA, the comparison is extended to the OAM-modes 5 and 6. Moreover, the CUCA, which has been most popularly considered in references, is specifically investigated to show the challenges of multiplexing implementation and the significance of the optimization of array parameters.

From our studies a range of observations with respect to design and performance of OAM systems are derived, which are summarized in Section V of concluding summary.

The remainder of this paper is structured as follows. A brief review is first provided in Section II for OAM-wave generation using antenna arrays. Next, the KPIs for OAM-generating arrays are addressed in Section III. Then, in Section IV, the feasibility of generating OAM using USA, UCA,

HCA and HCSA is firstly demonstrated, followed by the comprehensive performance study and comparison of these arrays based on simulation results. Then, the impacts of the number of array elements on KPIs, challenge of generating OAM-beams of higher modes, and the impact of the number of samples from phase-profile on purity are investigated. Moreover, CUCA is specifically investigated in terms of its capability of multi-mode OAM-beam generation and corresponding performance. Finally, the paper provides the concluding summary and further research issues in Section V.

II. OAM GENERATION BY PHASED ARRAYS: A REVIEW

Antenna arrays can be used to generate OAM-carrying wavebeams, which are simply referred to as OAM-waves or OAM-beams. This has been regarded an efficient method in terms of the complexity of implementation and hardware's physical size [6]. In principle, various types of antenna arrays may be employed to generate OAM-beams, including linear [16, 24, 55–58], planar square [20, 59–63], circular [19, 48, 49, 54, 64–75], three-dimensional (3D) helical [76], cylindrical and conical [77] and other 3D [76–80] arrays. Below, six types of antenna arrays are elaborated associated with their applications for generation of OAM-waves.

Before addressing the specific antenna arrays for OAMbeam generation, first, it is noteworthy that OAM has been studied with MIMO antennas, referred to as the OAM-MIMO [13, 55, 81]. The performance of OAM-MIMO systems has been studied and compared with that of the conventional MIMO systems in several references. More explicitly, in [55], the capacity and energy efficiency of the OAM-MIMO systems without specifying antenna structures were studied in multipath propagation scenarios. By exploiting the diversity of OAM-waves carrying different modes rather than relying solely on their orthogonality, the studies in [24] demonstrated that OAM-MIMO is capable of offering a superior capacity in comparison with the traditional MIMO. This superiority becomes more pronounced as the number of elements of an antenna array increases, or as the element spacing decreases. OAM-MIMO can also be configured to implement the OAM spatial modulation (OAM-SM) in millimetre wave communications, as done in [82], where the capacity, average bit error rate (BER) and energy efficiency of the OAM-SM systems were investigated. The studies conclude that the OAM-SM can be a promising scheme enabling energy-efficient communications. Specifically, this method allows to achieve an energy-efficient that can be more than 200% higher than that of the normal OAM-MIMO. Consequently, OAM-SM may be beneficial to relatively long-range communications.

In [57], the BER performance of a type of OAM-MIMO, referred to as the plane spiral OAM, was studied in line-of-sight (LoS) scenarios. The extension to non-line-of-sight (NLoS) cases was considered in [58]. Later in [16], an antenna structure originally employed in [56] was considered, based on which the capacity of OAM-MIMO systems was numerically analyzed when taking account of the spatial-energy dis-

tribution of the OAM-waves. Similarly, the antenna structure proposed in [56] was employed in [23], to address the impacts from atmospheric turbulence and the misalignment between transmit and receive antennas on the performance of OAM-MIMO systems. Specifically in [23], the BER and capacity performance of OAM-MIMO systems were studied. Accordingly, an optimization algorithm was proposed to enhance the performance of OAM-MIMO systems.

In the following, we review several types of antenna arrays that have been studied for the generation of OAM-waves. Note that, to implement these arrays, either tunable delay lines or phase shifters may be employed to control the phase delays required by different array elements to generate given OAM modes [83]. However, in our forthcoming discussion, it is assumed that phase shifters are used, owing to that this technique does not require feeding networks. Besides, it is assumed that signals are fed to the centers of the patches of array elements via coaxial cables, as this type of feeding is relatively easy to manufacture and matching, which also generates low spurious radiation [84].

Furthermore, we note that, while full-digital beamforming techniques have mainly been considered in research, hybrid beamforming techniques may also be employed to generate OAM-beams [27, 85–88]. Specifically, in [27, 85–87], the hybrid beamforming assisted OAMs have been studied from a far-field perspective. By contrast, in [88], an OAM scheme with the beamfocusing relying on hybrid beamforming is proposed for application in near-fields. Note furthermore that, in [85], the beam purity is investigated, and in [87], the directivity is addressed.

A. LINEAR ARRAY

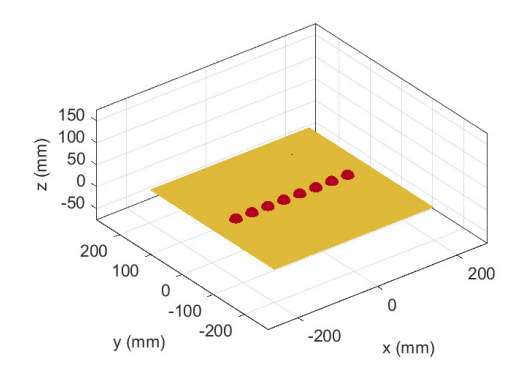


FIGURE 1: Illustration of uniform linear array (ULA).

A linear antenna array arranges its array elements along a line, typically with an equal spacing between two adjacent elements, forming the so-called uniform linear array (ULA), as shown in Fig. 1 [84]. Due to this linear geometric structure, linear arrays are only usable for generating OAMwaves, when individual array elements are independently

configured to generate OAM-beams, as discussed in [56]. The authors demonstrated that the travelling wave antennas can be employed to generate double-mode OAM-beams, which can simultaneously propagate coaxially with high isolation. To the best of authors' knowledge, except [55], all the other references [16, 23, 24, 57, 58, 82] on the linear arrays for OAM generation have followed [56] and assumed the travelling wave antennas. This is the consequence that, as above-mentioned, each array element has to be independently configured for generating an OAM-beam. Furthermore, so far, there are no published research results considered to generate OAM-waves using the linear arrays implemented by microstrip techniques. A possible reason is that linear arrays are hard to be built to effectively generate the phase-closed loop signals, which satisfy the periodic circulation property required by OAM-waves. Owing to the above-mentioned issues, linear arrays will not be specifically analysed in the forthcoming discourses of this paper.

B. UNIFORM CIRCULAR ARRAYS (UCA)

Parameter	Value
Number of Elements (N)	16
Phase Shift $(\phi_n, n = 1,, N)$	$2\pi l(n-1)/N$
Rectangular Radiator Dimensions	$0.02m \times 0.02m$
Feeding Width & Length	0.002m
Ground Plane Length & Width	0.4m

TABLE 1: An example of structure parameters for UCAs.

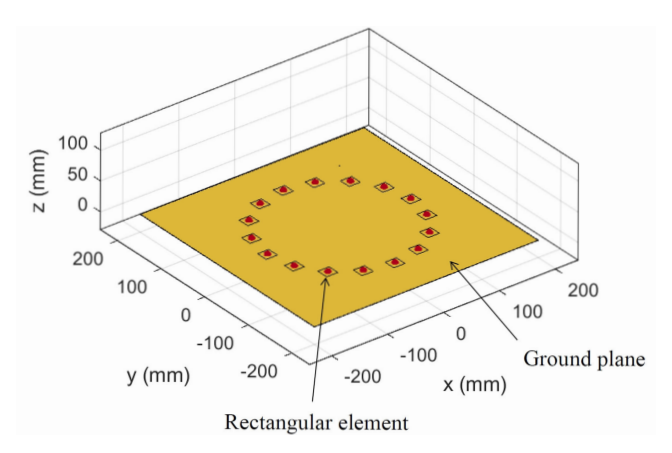


FIGURE 2: Illustration of uniform circular array (UCA), where the red-colored dot in each squared radiating element represents a signal feeder.

The UCA with radiating elements arranged on a ring constitutes a structure that is beneficial for OAM-wave generation in RF and, hence, has drawn a lot of research interest [48, 49, 63–67, 73, 89, 90]. A schematic of UCA is depicted in Fig. 2, with the array structure parameters, for example, shown in TABLE 1. To generate an OAM-wave of a given mode using a UCA, each array element is fed a signal with a specific phase in the azimuth direction [75, 91]. Assume that the N elements of a UCA are regularly indexed as n = 1, 2, ..., N, then, their phases can be activated according to [21, 92, 93]

$$\varphi_n^{(l)} = \varphi_0 + \frac{2\pi(n-1)l}{N},\tag{1}$$

for OAM-mode $l=\pm 1,\pm 2,\ldots$ In (1), φ_0 denotes the initial phase usually set to zero. Note that, although mathematically l can be any positive or negative integer, the maximum mode, denoted as $\pm l_{\rm max}$, which is meaningful in practice, is limited. According to [8, 49, 72, 94], the practically meaningful modes are integers falling in the range of $-N/2+1 \le l \le N/2-1$. Hence, we typically have $l_{\rm max}=N/2-1$, as evidenced by our simulation results in Section IV.

As indicated by (1), to generate an OAM-wave, an equal phase shift of $2\pi l/N$ is gradually added to the N array elements, from n=1 to n=N. This arrangement is desirable because of its simplicity in feeding signals into array elements and its feasibility for wavefront manipulation [95]. Moreover, as noted in [14,96], UCA is efficient, low-cost, and has a simple structure.

For fabrication of UCAs for OAM generation, microstrip patch array elements are typically utilized [48, 49, 63–67, 73, 89, 90], while this has not been used in [54, 72, 74]. Specifically, in [54, 72], dipole arrays were employed, while in [74], the spiral array was introduced. Additionally, in [73] and [97], one extra element positioned at the centre of UCAs was employed to transmit a beam of mode 0. Note that, as mode 0 wave is a traditional plane wave, which does not require an array to generate.

As mentioned above, radio frequency based OAM has been widely investigated with UCAs. Specifically, in [48, 64, 65, 73, 98], the OAMs of single mode operating in specific frequency bands were considered. In [68, 99], the single-mode OAM-waves at dual frequency bands were generated. The authors detailed both the design and configuration of radiators to generate the OAM-wave of a particular mode, where the performance was studied via numerical simulations and also verified by experimental results. By contrast, in [49, 54, 66, 67, 69, 72, 74, 100], the OAM-waves consisting of mixed modes were generated, where each OAM-mode was generated by a separate UCA with 8 array elements.

Furthermore, there has been a range of researches on the concept of mode division multiplexing implemented using the OAMs generated by UCAs. More specifically, in [15, 18, 49, 101, 102], it was demonstrated that if a superposition signal whose component signals are appropriately phase shifted is fed into the elements of a UCA, OAM-MDM can be achieved. In [15], the properties of OAM-MDM were exploited to achieve physical layer security for communications over wiretap channels. It was shown that the divergence and spiral phase properties of OAM-waves enable the design of wireless communications systems with new degrees of freedom for enhancing their secrecy performance. Based on UCA, in [101], a Butler matrix circuit was presented for generating the OAM-wave multiplexing several OAM-modes.

There are also various challenges for employing UCAs to implement OAM-MDM. First, in [18], three important concerns in OAM-MDM, including beam divergence, mode-

dependent performance deterioration, and degradation of receive signal-to-noise ratio (SNR), were addressed. Second, for a UCA to generate OAM-MDM wave, a specifically designed feeding network is required, which lacks the steering flexibility [83]. Besides, the OAM-beams carrying high-order modes become severely divergent, which may yield considerable attenuation of the received signal, when the same sampling plane at the receiver is employed. In this case, it is not feasible to increase the capacity of UCA-MDM systems via multiplexing the OAM-modes of high-orders. Instead, to improve the capacity provided by OAM-MDM, it is more promising to replace UCA by the concentric UCA (CUCA) [14, 83], which consists of multiple rings of arrays with each ring being a UCA for generating one OAM-mode, as further explained in Section II-D.

C. UNIFORM SQUARE ARRAY (USA)

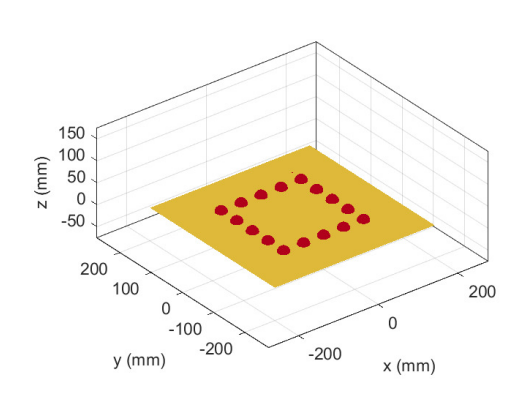


FIGURE 3: Schematic of uniform square array (USA).

USAs, as shown in Fig. 3, belong to a special class of rectangular arrays, where antenna elements are uniformly positioned along a square grid [84]. Several USAs have been studied with OAM [59–62], showing that USAs can be employed to generate OAM-waves similarly as UCAs, but by feeding antenna elements with the unevenly distributed phases according to the elements' azimuth angles. Specifically, assume a USA with the number elements expressed as N = 4N'. Let the center of the USA be the origin of a Cartesian coordinate system, and let the coordinates of the N array elements be (x_n, y_n) , n = 1, 2, ..., N, labelled in anti-clock direction. Furthermore, assume that (x_1, y_1) is the first element in the first quadrant, while (x_N, y_N) is the last element in the fourth quadrant. Then, for generating mode l, $l = \pm 1, \pm 2, ...$, the phase shifts fed into the array elements

can be expressed as

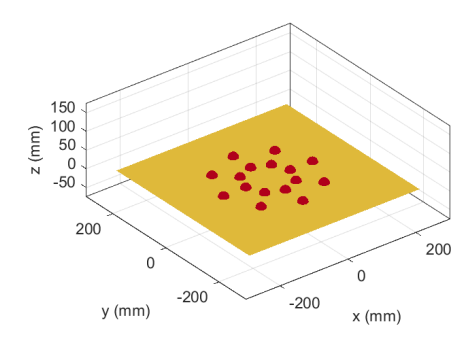
$$\varphi_n^{(l)} = \begin{cases} \varphi_0 + \arctan\left(\frac{y_n}{x_n}\right)l, & n = 1, \dots, \frac{N}{2}, \\ \varphi_0 + \left(\pi + \arctan\left(\frac{y_n}{x_n}\right)\right)l, & n = \frac{N}{2} + 1, \dots, N, \end{cases}$$
(2)

where $0 \le \arctan(y_n/x_n) < \pi$ was defined and φ_0 is a common initial phase. Notice in (2) that the phase differences between two adjacent elements are not always the same.

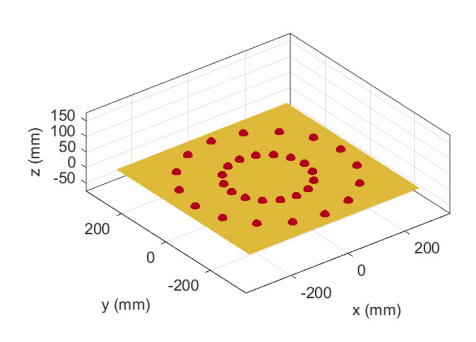
In [59], a 4×4 USA-based OAM scheme was introduced for operation in indoor multipath environments, with the aim to enhance the throughput of WiFi. The results demonstrate that OAM-MIMO outperforms the corresponding traditional MIMO, regardless of whether the water-filling power allocation or the equal power allocation is applied. The OAM schemes based on the general rectangular arrays were studied in [60]. It is shown that the capacity attainable by an OAMconfiguring rectangular array system can be significantly higher than that by a traditional MIMO system of the same antenna structure. In [61], USA was used to generate OAM vortex beams, showing that the peak-to-sidelobe ratio can be significantly increased. For example, by disabling one-fourth of the antenna elements of a USA with 64 elements with the aid of a sparse 2D array genetic algorithm, more than 8 dB of sidelobe reduction can be attained. In [62], with the aid of the Hankel transform [103, 104] for aperture antennas, the studies demonstrate that a USA may be configured to generate either a higher gain or a wider beamwidth, when compared with a UCA. Moreover, when the same aperture area is assumed for both UCA and USA, it is shown that the weighting coefficients for the array elements of a USA can be adjusted to attain an antenna gain that can be larger than the gain of a UCA. However, in the above-mentioned references for USA, the beam pattern and purity performance were not investigated. Based on our results presented in Section IV, the high directivity of USA is at the cost of low purity. Furthermore, whenever a USA yields better directivity than a UCA, the corresponding beam pattern of USA fails to obtain the hollow doughnut-shaped characteristics required by OAM, as seen, for example, in Fig. 14a.

Additionally, there are some researches considered the OAM schemes using a USA of four elements [20, 105, 106]. In this case, the USA is a UCA with an azimuth phase interval of 90 degrees. Explicitly, a four-patch antenna array was designed in [20] for generating the OAM-waves of Mode ± 1 , which claimed to achieve the purity as high as 97%. However, it is also shown that the transmission distance and sampling radius at the receiver impose impact on the attainable purity. In [63], both a 4-element USA and an 8-element UCA were proposed for OAM generation, and their transmission characteristics and beam purity performance were compared. The studies verify that increasing the number of array elements improves the purity performance of OAM-waves, which is consistent with our simulation results detailed in Section IV of this paper.

D. CONCENTRIC UNIFORM CIRCULAR ARRAY (CUCA)



(a) 8 elements on each ring.



(b) 16 elements on each ring.

FIGURE 4: Schematic examples of concentric uniform circular arrays (CUCA).

Most concentric arrays are implemented based on a circular topology consisting of multiple rings of UCAs, as shown in Fig. 4. Hence, they are referred to as CUCAs. With this topology, the phases of different elements on a ring of sub-array can be activated according to (1) to generate a specific OAMmode. Different rings of sub-arrays can be set to generate the same mode or different modes. Furthermore, all the elements on different rings of sub-arrays can be configured to jointly generate OAM-waves carrying multiple OAM-modes.

There are other array structures also classified as concentric arrays. For example, in [107], an array with eight concentric spiral sub-arrays was introduced, so as to generate three OAM-modes for operation in a frequency band higher than 1 GHz. The concentric array with multiple spiral sub-antennas was also considered in [108].

CUCA has some unique characteristics and advantages for applications. First of all, the arrangement of multiple rings of sub-arrays enables to deploy more antenna elements in a given area, when compared with the UCA of one ring. Owing to this structure, flexible beam patterns and OAM-

IEEE Access

References	No. of elements on rings (from inner to outer rings)	Alignment of elements on different rings
[17, 109–111]	Same	Yes
[83, 112–114]	Linearly increases	No
[11, 52, 108, 115]	Non-linearly increases	No

TABLE 2: Examples of CUCA structures with antenna elements on different rings arranged in different ways.

modes can be generated [116–119]. The excitations of individual elements of a CUCA can be optimized to improve the beam focusing, or to generate the superposition signals carrying multiple OAM-beams of both positive and negative modes [52]. Consequently, the spectral efficiency of communication can be improved with the aid of, such as, OAM-MDM [120].

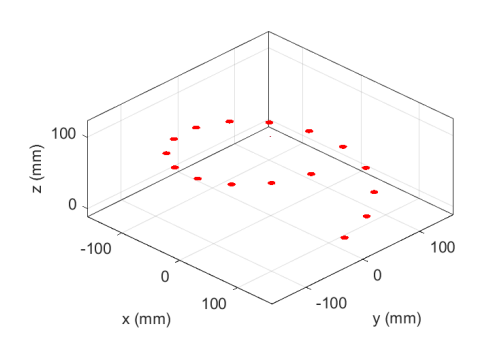
Specifically, in comparison with UCA and assuming the same number of antenna elements, CUCA may have a higher complexity for fabrication, while it has a higher flexibility for design [121]. With UCA, the array elements are equally arranged on one ring, which results in relatively big aperture size. By contrast, for a CUCA, the numbers of array elements on different rings of sub-arrays may be different, and the array elements of one ring can be flexibly positioned at different locations. For example, in [17], the CUCA is structured to make all the rings have the same number of antenna elements, and the antenna elements are positioned to form multiple linear sub-arrays spanning a full circle in the azimuth plane. It is shown that this structure is beneficial to generating pencil-like beams. Alternatively, the antenna elements on different rings can be positioned with relative rotations to obtain a dense CUCA structure [14, 83, 113–115]. This CUCA structure has the advantages for generating both integer and fractional OAM-modes, providing implementation flexibility to meet the radiation characteristics for specific applications [113], and for simultaneously generating multiple OAM-modes with good mode isolation [114]. Furthermore, different rings may be assigned different numbers of antenna elements, allowing a CUCA structure with nearly uniformly distributed antenna elements in the azimuth plane [83, 112]. To summarize, TA-BLE 2 shows three types of CUCA structures, where "same" means that different rings of sub-arrays have the same number of antenna elements, and "aligned" indicates that the array elements on different rings are aligned to form multiple linear sub-arrays.

The CUCA-based OAM has been investigated with different consideration. For example, in [14], the authors designed the CUCA-based OAM to simultaneously transmit multiple parallel low-order OAM-modes to improve the capacity. Accordingly, considering two cases of, namely, co-mode-interference-free and co-mode-interference, the authors proposed the corresponding mode-decomposition schemes for signal detection. Furthermore, optimal power allocation across different OAM-modes was studied. In the OAM-carrying waves generated, such as, by UCA or USA, the radiation density peaks of different modes have different locations, making wireless transceiver design practically chal-

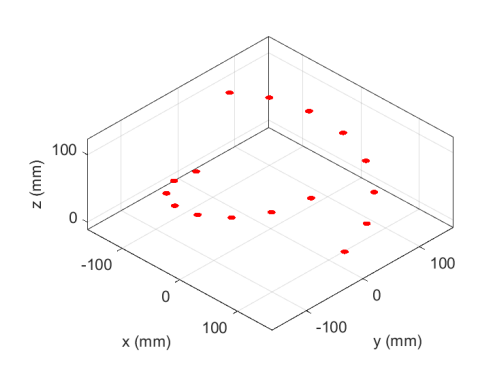
lenging. CUCA is capable of providing a solution for this peak location inconsistency problem [117, 122]. Specifically, by exploiting the property that the divergence angle of an OAM-beam of a given mode is a function of the radius of the transmit UCA generating the OAM-beam, it is possible for the OAM-beams carrying different modes to focus on one receive ring for signal sampling. Consequently, at the receiver, similar power can be acquired for demodulating different OAM-modes, allowing to mitigate the problem of the mode-dependent performance [122].

Note that, similar to the UCA considered in [97], for the CUCA considered in [109], an antenna element can be placed at the center of the array to transmit a beam of mode 0.

E. THREE-DIMENSIONAL (3D) HELICAL ARRAY



(a) Schematic of HCA.



(b) Schematic of HCSA.

FIGURE 5: Examples of 3D antenna arrays for OAM generation.

So far, all the arrays introduced for OAM-wave generation have the planar structure, which need to set specific phase shifts for individual array elements, for example, by a phase shift network (PSN). Alternatively, by exploiting the propagation delay, the phase shifts required for different array elements may be generated from their relative physical

locations. In this case, the antenna array has a 3D structure. In [76], two types of 3D helical arrays were proposed, namely the helical circular array (HCA), as seen in Fig. 5a, and the helical circular sub-array (HCSA), as shown in Fig. 5b. Furthermore, in [123], the authors reported the fabrication and experimental validation of the HCAs proposed in [76]. To be more specific, in [123], an 8-element HCA is fabricated without employing the phased feeding network for generating OAM-mode $l=\pm 1,\ \pm 2,$ or ± 3 . The experimental results show that the fabricated HCA is capable of achieving the reflection coefficients less than 10 dB across different OAM-modes, and attaining a purity higher than 0.8 for all OAM-modes considered.

As above-mentioned, the geometric structures of HCA and HCSA allow to introduce the required phase shifts for array elements based on the space relationships of the array elements. This can be explained as follows. First, for a HCA of *N* total elements regularly indexed, the heights of the array elements of HCA is given by [76]

$$h_n = \frac{\lambda(N-n)l}{N}, \quad n = 1, 2, \dots, N,$$
 (3)

in the direction of propagation, which means that the decremental height between the *i*th and (i + 1)th elements is [76]

$$h_{decre} = \frac{\lambda l}{N},\tag{4}$$

where l is the OAM-mode number and λ is the wavelength. Then, when all elements are fed with an identical signal of frequency $f=c/\lambda$, the resultant relative phase shifts of the array elements are

$$\phi_n = \frac{2\pi(n-1)l}{N}, n = 1, 2, \dots, N,$$
 (5)

when they arrive at a plane perpendicular to the propagation axis. Explicitly, the azimuth angles of ϕ_n yielded by the array elements are identical to that in (1) for UCA.

Similarly, for a HCSA with its elements regularly indexed, the height of the (N - n)-th array element can be set to [76]

$$h_n = \frac{\lambda \left((N-n)_{[N/l]} \right) l}{N} + \delta(n),$$

$$n = 1, 2, \dots, N; N/l \in \mathbb{Z}^+,$$
(6)

where N/l is an integer denoting the number of elements per sub-array when l is the number of sub-arrays, $(\cdot)_{[\cdot]}$ is the modular operation, and

$$\delta(n) = \begin{cases} \frac{N}{l}, & \text{if } n_{[N/l]} = 0, \\ 0, & \text{otherwise.} \end{cases}$$
 (7)

From the above equations and also as shown in [76], with either HCA or HCSA, an OAM-mode is determined solely by the locations of the array elements, which are set based on the OAM-mode to be generated. Hence, in comparison with UCA, HCA allows to simplify the hardware requirements, as it does not include an extra PSN for setting the phases of array

elements. HCSA can further reduce array's physical size by using two or more spiralling sub-arrays.

As demonstrated in [76], HCA and HCSA are capable of achieving a gain of more than 10 dBi. However, a HCA or HCSA can only generate one OAM-mode determined by its fixed physical structure. In comparison with HCA, whose height increases linearly with the OAM-mode number l, the height of HCSA in fact slightly reduces with the increase of OAM-mode number l, if the number of spiral sub-arrays is designed to be equal to the OAM-mode number l, as illustrated in TABLE 3, where $h = h_{decre}$.

	Mode	Total height of HCA	Total height of HCSA
	1	$(N-1) \times h$	$(N-1) \times h$
ĺ	2	$(N-1) \times 2h$	$(N/2-1)\times 2h = (N-2)h$
ĺ	3	$(N-1) \times 3h$	$(N/3-1)\times 3h = (N-3)h$
ĺ	4	$(N-1) \times 4h$	$(N/4-1)\times 4h = (N-4)h$

TABLE 3: Aperture height comparison between HCA and HCSA [76].

While having the above-mentioned merits, the helical arrays for OAM generation have some shortcomings. First, as the OAM-mode is determined by the physical locations of the array elements, both HCA and HCSA are not flexible for generating the beams with different OAM-modes. Second, one array can only generate waves of one OAM-mode. Furthermore, as different array elements have different distances to a receiver, the helical arrays are only suitable for farfield applications, where the distances from different array elements to receiver can be nearly the same. They are not suitable for the near-field applications, where the distances from array elements to receiver have explicit differences. However, the research results in references [57,81] show that OAM-MIMO has little advantage over the conventional MIMO, when communicating in far-field communications scenarios.

Note that, instead of using HCA or HCSA implementation, while also free of a PSN, time-modulated arrays [124] can be implemented to generate OAM-beams. To generate a beam carrying a specific OAM-mode, different array elements become activated at the instants, which yield the phases as required for generating the expected OAM-mode.

F. OTHER ARRAYS

There are other types of arrays in addition to the above-mentioned, which have also been considered for OAM generation, including cylindrical, conical, and elliptical arrays. Specifically, cylindrical arrays were studied in [77] and [80]. In [77], conical array was introduced and compared with the cylindrical array, showing that it can increase diversity and provide feasibility for OAM-wave generation. The elliptical array was investigated in [50]. However, we should note that, except the above-mentioned references, these three types of arrays have so far rarely been considered elsewhere. Accordingly, they will not be considered further in this paper.

In TABLE 4, different types of arrays and the techniques for their implementation considered in literature are summa-

rized.

III. KEY PERFORMANCE INDICATORS AND SUBORDINATE ISSUES FOR OAM ANTENNA ARRAYS

The design of antenna arrays for conveying OAM, or simply OAM arrays, involves many metrics for explaining and demonstrating its performance. These metrics allow us to compare the performance between different designs. In literature, the performance comparison between different OAM arrays is not unified, but research-objective oriented, more or less, in an ad-hoc way. Therefore, in this section, we provide a comprehensive summary for the key performance indicators (KPIs) for OAM arrays, including directivity, maximum OAM-mode producible, multiplexing capability of OAM-modes, beam divergence angle and beam purity. Furthermore, some secondary metrics, namely cost, array size and hardware requirements are briefly discussed. In Section IV, different OAM arrays will be compared against the KPIs.

A. DIRECTIVITY

Directivity is one of the most important KPIs in the design of OAM arrays [127]. Directivity measures the strength of an array pointing its radiation in certain direction compared with that of an isotropic radiation with the same amount of transmit power [84]. Hence, directivity reflects the effectiveness of an array transferring energy in a specific direction [84, 128, 129]. Directivity can be measured by either absolute value or normalized value, depending on the applications. Specifically, when considering the coverage of an array, the absolute directivity is in its favour. By contrast, if the relationship between the main-lobe and side-lobes of an array is emphasized, the normalized directivity is preferred. In practice, both directivity measurements are often required in the design of antenna arrays.

As the directivity of different arrays is compared in the next section, the absolute directivity is considered in this paper, which can be evaluated from the formula [84]

$$D(\theta, \phi) = \frac{4\pi \left| Af(\theta, \phi) \mathbf{w}^H \mathbf{s} \right|^2}{P_{\text{total}}}, \tag{8}$$

where A is the nominal field amplitude, $f(\theta, \phi)$ is the normalised field pattern in terms of the elevation angle θ and azimuth angles ϕ , \boldsymbol{w} is the complex weight vector for the array, \boldsymbol{s} is steering (array manifold) vector, and P_{total} is the total radiation power of the array.

B. LARGEST PRODUCIBLE OAM-MODE

Largest producible OAM-mode (LPM) refers to the largest meaningful absolute OAM-mode that an array can generate. In theory, an array may generate an OAM-wave of any mode characterized by a positive or negative integer. However, when given an array and the number of array elements, the OAM-wave with its absolute mode number higher than a certain value may practically be of no use due to its poor performance, as discussed in Section IV. Also, in Section II-B, the largest distortion-less OAM-mode producible by

UCA has been explained. In practice, generating a perfect OAM-beam is often difficult. However, the property of an OAM-wave is still counted as long as it is not severely distorted. Typically, an OAM-wave of certain mode is regarded to be producible or discernible, if, in the OAM spectrum, the intensity of the target OAM-mode is at least twice of the intensity of the highest non-target OAM-mode. As shown by our results provided in Section IV, in general, UCAs or helical arrays can produce the OAM-waves of relatively higher quality than USAs, especially, when the OAM-waves with relatively high-modes are considered.

The LPM of some types of arrays is summarised in TABLE 5, which will be examined in detail in Section IV-A and Section IV-B.

C. CAPABILITY OF MODE DIVISION MULTIPLEXING

OAM multiplexing has the potential to increase the spectralefficiency via providing new methods for system design, such as, multiplexing of users or services. OAM-mode division multiplexing (OAM-MDM) can be regarded as a subcategory of spatial multiplexing. Hence, as spatial division multiple access (SDMA), OAM-mode division multiple access (OAM-MDMA) [3] may be implemented to support multiple users to transmit information on the same frequency band and at the same time. In other words, with OAM-MDM, a multiplexing vortex beam is capable of carrying several component OAMbeams with each conveying its own information, either to one receive terminal for a higher data rate or to multiple receive terminals in the principle of OAM-MDMA [130]. Furthermore, OAM-MDM can be integrated with other multiplexing techniques, including frequency division multiplexing (FDM), time division multiplexing (TDM) and space division multiplexing (SDM), for supporting various types of services with different quality-of-service (QoS) requirements.

Hence, the capacity of an OAM system is dependent on the number of modes concurrently available [6]. As mentioned in Section II-B, UCA can implement OAM-MDM by feeding the superposition signals carrying several OAMmodes. However, for OAM-MDM implementation, UCA is less flexible than CUCA, as a CUCA enables its different rings of sub-arrays to generate the OAM-waves of different modes. Similar to UCA, USA can also implement OAM-MDM, but its number of usable modes is usually smaller than that of UCA, when considering the same total number of array elements, as concluded in Section IV-B and Section IV-C. The 3D helical arrays, including HCA and HCSA, are the least flexible ones for OAM-MDM implementation, as the OAM-modes generated by this type of arrays are determined by their physical structures, which are hard to be reconfigured for generating the OAM-waves of different modes in practice.

D. BEAM DIVERGENCE ANGLE

A special feature of OAM-waves is its radiation profile shaped like a doughnut with almost zero radiation power in the center, when sampled on a plane perpendicular to the propagation axis [11, 131]. An OAM-beam tends to diverge

Array Type	Implementation Technique	References
-	Travelling-wave ring resonator with parabolic reflec-	[56]
	tor	
Square	Microstrip	[105], [20]
Square	Helix	[106]
Square	Omnidirectional (isotropic)	[61]
Circular	Microstrip (Square, Rectangular or Circle)	[48, 49, 63–67, 73, 89, 90]
Circular	Microstrip Yagi	[68]
Circular	Microstrip slot	[71]
Circular	Dipole	[54, 72]
Circular	Microstrip spiral	[74]
Circular	Pyramidal Horn	[19]
Concentric	Microstrip (Square, Rectangular or Circle)	[11, 17, 51, 52, 83, 110, 125]
Concentric	Microstrip slot (Compact Archimedean)	[108]
Concentric with centre element	Not mentioned	[109]
3D	Helix	[78]
3D circular	Vivaldi antenna	[79]
3D circular	Microstrip	[80]
3D helical circular	Microstrip	[76]
3D-cylindrical and conical	Microstrip	[77]
Elliptical	Microstrip	[50]
Discrete spiral & concentric	Microstrip	[116]
Luneberg Lens	Microstrip	[97]
Parabolic antenna	Microstrip	[126]

TABLE 4: Different types of arrays with implementation techniques for OAM-wave generation.

Array Types	LPM (l_{max})
USA	$-\frac{N}{2}-1 < l_{max} < \frac{N}{2}-1$
UCA	$-\frac{N}{2} < l_{max} < \frac{N}{2}$
HCA & HCSA	$-\frac{N}{2} < l_{max} < \frac{N}{2}$

TABLE 5: LPM for USAs, UCAs and HCA/HCSA.

while propagating, and the divergence effect becomes severer with the increase of the absolute mode number l [131, 132]. This property results in that the power of an OAMbeam carrying a relatively higher mode progressively diffuses as the transmission distance increases. Consequently, from a given sampling area, the available signal power dramatically reduces, resulting in significant degradation of receive SNR, when compared with the conventional beams of wellsteered [131, 133]. Therefore, it is challenging to employ OAM-beams, especially those carrying high OAM-modes, for supporting long-distance communications [133]. When the communication distance increases, more antenna elements are required for the receiver to accumulate sufficient energy for information detection [11]. Furthermore, due to the intrinsic divergence property of OAM-beams, the size of receive antenna array, such as a ring of array for receiving signals sent by UCA, may need to increase as the transmission distance increases [133], which is surely impractical for mobile communications. To mitigate this problem, an OAM transmitter is required to be carefully designed, allowing OAM-beams to be capable of concentrating within a compact range. Accordingly, a relatively high SNR can be attained within certain transmission range required by the specific application scenarios [131].

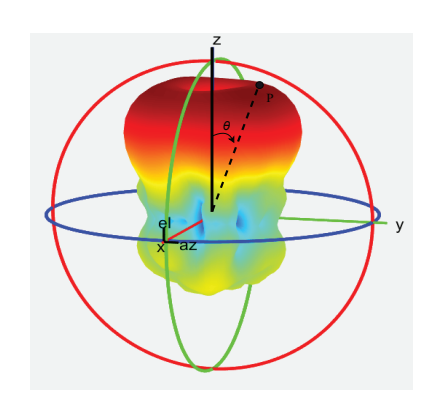
To be more specific, as to be detailed in Section III-E, in OAM systems, spatial sampling is usually performed by antenna arrays to obtain the received signals for information

recovery [134]. From the above-mentioned, as the transmission distance increases, the vortex beam of a given OAMmode increases, possibly resulting in an intolerably large size of the antenna arrays implementing sampling on the entirecircles [135]. To mitigate this problem, in [136], a partial arc sampling receiving (PASR) scheme was proposed, which enables significant reduction of the size of OAM receive antennas. Specifically, the PASR method only requires to sample a portion of the full 2π circle, and hence, enabling significant reduction of array size. The studies in [136] show that a receive array sampling over an arc of $\pi/2$ only results in slight performance loss in comparison with that sampling a whole circle of 2π . By contrast, in [137], the OAM-beam divergence problem was handled with via appropriate excitation of the individual elements of transmit array, to focus the OAM-beam onto a receive array of small and fixed size.

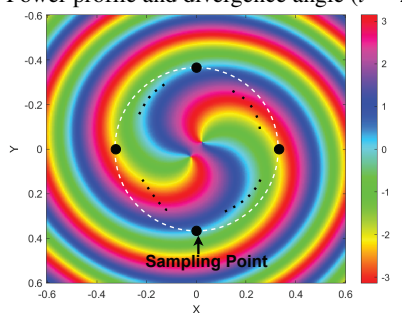
Explicitly, the divergence angle of an OAM-beam is an important metric reflecting the characteristics of the antenna array generating the OAM-beam. To measure the divergence angle of an OAM-beam, the Poynting vector can be used to represent the directional energy flux or power flow of the OAM-beam's electromagnetic (EM) field [138]. Assume an OAM-beam propagates in the positive direction of the z-axis, the Poynting vector is defined as the one perpendicular to the helical wavefront. In this case, the angle θ , as shown in Fig. 6a, of the Poynting vector with respect to the positive z-axis direction is known as the divergence angle from the first principle [132]. According to this definition, the divergence angle is given by the angle between the beam's propagation direction and the direction yielding the maximum directivity [11, 139–143].

Note that in literature, there are some slightly different definitions for divergence angle. For example, in [46, 97], the divergence angle was measured as the angle between the *z*-

axis (positive direction) and the far-side tangent to the OAM-beam. In [144], the divergence angle was considered as the open angle of the OAM-beam symmetric to the *z*-axis, which is hence twice of the angle given by the first definition. In this paper, the first definition of divergence angle is utilized, since it has been widely used in the literature.



(a) Power profile and divergence angle (l = 2).



(b) Phase profile and sampling (l = 2).

FIGURE 6: Power profile and phase profile of a UCA with 16 elements.

E. MODE PURITY OF OAM BEAM

In an OAM-beam, the intensity of a desired OAM-mode relative to the total intensities of all modes in the beam is regarded as the OAM-mode purity or referred to the OAM spectrum [145, 146]. Mode purity is one of the important characteristics of OAM-waves. In practice, OAM-beams are not ideally pure, meaning that they do not necessarily have perfect helical distributions. Different OAM-modes may not be ideally orthogonal with each other. This may be the result of different factors in practice. First, antenna misalignment and multipath effects lead to imperfect circulant channel matrix between, e.g., two UCAs. Consequently, the channel matrix cannot be correctly diagonalized by the discrete Fourier transform (DFT) processing. As the result, the power of an OAM-mode leaks into its adjacent modes, yielding inter-mode interference (IMI) [19, 20, 86, 147]. Second, IMI may occurs even in the ideal line-of-sight (LoS) transmission condition. For example, in mobile application scenarios, turbulence introduces phase noise, which may interrupt the orthogonality between OAM modes, resulting in energy leakage into adjacent modes via harmonic expansion [148]. This effect becomes severer with the increase of propagation distance and/or turbulence strength.

Some methods have been proposed to mitigate IMI. Specifically, in multipath environment, spatial-domain equalization may be implemented to suppress IMI [135]. By contrast, beam-steering-based methods can be designed to effectively overcome the misalignment between transmit and receive arrays [121].

OAM-mode purity can be examined from the standpoints of either the helical harmonic expansion or the rotating operator of quantum mechanics in optical field [130]. In RF scenarios, the purity of OAM-beams can be estimated with the aid of the Fourier transform, which facilitates spectrum analysis and hence, the OAM-mode decomposition [8, 19]. Specifically, as shown in Fig. 6b, using the circular phase profile of $\Psi(\phi)$, $-\pi \le \phi \le \pi$, we have [149, 150]

$$A_{l} = \frac{1}{2\pi} \int_{-\pi}^{\pi} \Psi(\phi) e^{-jl\phi} d\phi,$$

$$\Psi(\phi) = \frac{1}{\sqrt{2\pi}} \sum_{l=-\infty}^{\infty} A_{l} e^{jl\phi},$$
(9)

where A_l are the Fourier coefficients with $|A_l|^2$ denoting the power of different OAM-modes. Then, the purity of the lth OAM-mode can be evaluated as [23]

$$P_{u}(l) = \frac{|A_{l}|^{2}}{\sum_{i=-\infty}^{\infty} |A_{i}|^{2}} = \frac{|A_{l}|^{2}}{E[|\Psi(\phi)|^{2}]},$$

$$l = \pm 1, \pm 2, \dots,$$
(10)

In computation of (9), $\Psi(\phi)$ is given by its sample values along a circle as shown in Fig. 6b. In this case, the Fourier transform in (9) needs to be replaced by the DFT. In detail, let $\Psi(\phi_0), \Psi(\phi_1), \dots, \Psi(\phi_{N-1})$ be the N samples obtained in $[-\pi, \pi]$ of the phase profile. Then, the DFT coefficients are given by

$$A_l = \frac{1}{N} \sum_{i=0}^{N} \Psi(\phi_i) e^{-jl\phi_i}, \ l = 0, \pm 1, \dots, \pm l_{\text{max}},$$
 (11)

when $2l_{\text{max}} + 1 \le N$ OAM-modes are considered. Accordingly, (10) is modified to

$$P_{u}(l) = \frac{|A_{l}|^{2}}{\sum_{i=-l_{\text{max}}}^{l_{\text{max}}} |A_{i}|^{2}} = \frac{|A_{l}|^{2}}{E[|\Psi(\phi)|^{2}]},$$

$$l = \pm 1, \pm 2, \dots, \pm l_{\text{max}}.$$
(12)

F. SUBORDINATE ISSUES

In addition to the KPIs considered so far in this section, there are some subordinate issues, which may need to be aware of in the design of OAM arrays. Below, three issues are briefly introduced, including the peak-to-sidelobe ratio (PSLR), phase shift network (PSN), as well as operation frequency and array size.



1) Peak-to-Sidelobe Ratio (PSLR)

Sidelobes are unavoidable for any directional antennas, which are closely related to the diffraction effects of radio waves. When there are sidelobes, an antenna array radiates energy in unwanted directions in addition to the desired main-lobe direction [151]. Hence, numerous methods have been proposed to minimise sidelobe levels [152]. Typically, PSLR, which is given by the ratio between the power of main-lobe and that of maximal sidelobe, is used to quantify the severity of sidelobes [153]. One of the aims in array design is to suppress sidelobes for a highest possible PSLR, typically, a value of more than 10 dB [154].

Besides PSLR, the angle at which a sidelobe occurs is also crucial. If a sidelobe is close to the main-lobe, it may result in a large energy loss. The situation can be more complicated and unexpected, as the array's size and the number of array elements increase [63].

2) Phase Shift Network (PSN)

A classic planar array requires a PSN or the structure of its kind to generate and detect OAM-beams [15,53], as mentioned in Section II-E. A transceiver generating multiple OAM-modes needs an array with multiple RF chains, PSNs, and power splitters or combiners, which is usually expensive and energy-greedy [29]. As explained in Section II-E, the 3D helical arrays can generate OAM-waves using their geometric structures [76]. However, this type of OAM arrays require more spaces than planar arrays. In [124], time-modulated UCAs were proposed for OAM-wave generation, which do not rely on PSNs. This might be a promising approach but requiring further research.

3) Array Size and Operation Frequency

It is well-known that the aperture size of an antenna array is inversely proportional to the operating frequency. A higher frequency corresponds to a smaller wavelength, and thus a reduced array size if the same number of array elements is considered. In some application scenarios, array size is not critical. For example, at BSs or ground stations, antenna arrays can be relatively large. In contrast, due to the highly crowded internal components required to support numerous functions, the arrays embedded in mobile terminals are highly challenging to implement in cm-wave and even in mm-wave [155]. In the design of antenna arrays, size optimization, in particular, in the case of relatively low operation frequencies, is critical for reducing the size of antenna arrays [156]. This becomes predominant when miniature antennas operating with wideband or multiple frequency bands are designed [157].

IV. PERFORMANCE COMPARISON OF OAM ARRAYS

In Section II, the typical types of OAM arrays have been reviewed, including linear array, UCA, USA, HCA, HCSA and CUCA. In Section III, the KPIs of antenna arrays for the OAM-based communications are identified and briefly explained. Based on simulation results, in this section, we compare the performance of OAM arrays against the KPIs,

so as to reveal the comparative advantages and disadvantages of the various OAM arrays as considered.

Note that, from TABLE 4 we can observe that microstrip patch antennas are preferred for OAM-beam generation, owing to their compact size, low manufacturing cost, and comparatively simple structure [41,158]. Hence, in this section, all OAM arrays are assumed to be implemented by the microstrip technique. Additionally, as mentioned in Section II-A, linear OAM arrays have only been studied in the context of travelling wave antennas, but not with the microstrip patch antennas. For this reason, linear array is not included in the following performance comparison.

More explicitly, in this section, the directivity, LPM, divergence and OAM-mode purity of UCA, USA, HCA, HCSA and CUCA are compared. Before the comparison, first, in Section IV-A, the feasibility of using UCA, USA and HCA and HCSA for OAM generation is examined, followed by some assumptions and explanations made for the following performance comparison. Next, in Section IV-B, the performance of four types of arrays, namely UCA, USA, HCA and HCSA, is compared when the OAM-modes from 2 to 4 are considered. Then, in Section IV-C, considering both USA and UCA, we demonstrate the impact of the number of array elements on the performance of these two arrays. Then, in Section IV-D, the USA and UCA generating relatively high modes, including 5 and 6, are studied in terms of the LPM and mode purity. Finally, in Section IV-E, the purity of CUCA is studied.

A. PARAMETERS SETTINGS, ASSUMPTIONS AND FEASIBILITY EXAMINATION

According to [63], an array's feasibility for OAM generation can be examined based on its vortex phase profile, null in OAM-beam center and the doughnut shape intensity. To examine the feasibility, below we consider the arrays with 16 elements to generate OAM-beams of mode 1.

Array Type	Radius/	Observation Distance	GP Length/
(No. of Elements)	Length (m)	from Array (m)	Width (m)
UCA (8)	0.06533	0.273	0.6
UCA (12)	0.09659	0.597	0.6
UCA (16)	0.12815	1.051	0.6
UCA (24)	0.19153	2.348	1.4
USA (8)	0.1	0.273	0.6
USA (12)	0.15	0.597	0.6
USA (16)	0.2	1.051	0.6
USA (24)	0.3	2.348	1.4

TABLE 6: Simulation parameters for USA and UCA.

As argued in [84], to avoid grating lobes, the spacing of array elements must be less than $\lambda/2$. When the spacing of array elements is larger than $\lambda/2$, the mutual coupling effect of elements can be alleviated or ignored [84]. Therefore, in our study, the element spacing is set to $\lambda/2$. To carry out fair comparison between different arrays, all phase profiles are observed at a distance (in propagation direction) equating 0.8 times the Rayleigh distance, i.e., $0.8 \times (2D^2/\lambda)$, from the arrays, where the amount in bracket is the approximated

Rayleigh distance, when assuming that the arrays largest dimension D is larger than the wavelength λ [84]. Therefore, in our simulations, we assume that the number of array elements is at least 8. For all arrays, we assume a ground plane (GP) [129] having certain area. Note that, GP is a planar (or similar) horizontal conducting surface, which is functioned as a component of an antenna array, responsible for reflecting the radio waves emitted by antenna elements [129]. In Table 6, the parameters, including array radius and length, GP size and observation distance, for both UCA and USA are summarized, where '(m)' represents meter. Some other global parameters used in our simulations for defining array elements are listed in TABLE 7.

Note that, the parameters for HCA are identical to those for UCA, except that the GP size is zero and the elements' height increment is 0.07 metres. Similarly, the parameters of HCSA can be set, as listed in TABLE 3.

Throughout the comparison in this section, the following assumptions and settings are applied. First, to illustrate the directivity and divergence angles of arrays, we assume that the centers of arrays are positioned at the origin of the xyplane, while waves propagate in the positive z-axis direction, for example, as shown in Fig. 7c. Second, as for the 3D helical arrays, no GP is considered, as it is unrealistic for them to use GP. However, to carry out a fair comparison, the performance of 3D helical arrays is compared with that of a UCA without GP. Third, all phase profiles are demonstrated with the same resolution of 5 millimetres (mm). Finally, in the cases of OAM-modes 1 to 4, we set the size of the observation plane to be $0.6 \text{ m} \times 0.6 \text{ m}$. By contrast, in the cases of OAM-modes 5 and 6 in Section IV-D generated by an array with 24 elements, the larger observation areas of 1.2 m \times 1.2 m and 1.4 m \times 1.4 m are applied, respectively.

Based on the above-mentioned assumptions, the performance of different antenna arrays set to generate different OAM-modes is evaluated as follows.

First, in terms of the simulation framework and numerical methodology, antenna arrays were implemented using the Method of Moments (MoM) provided by Matlab's 'Antenna Toolbox'. The method solves Maxwell's equations via the surface discretization of antenna structures into triangular mesh elements, based on which surface currents and electromagnetic fields are iteratively calculated, until convergence is achieved.

Second, the directivity and divergence angle of an antenna array can be estimated from the following implementation consisting of six key stages:

- Geometrical definition of the rectangular patches with dimension-optimized feeding ports.
- Implementation of antenna array via the 'Antenna Toolbox' of Matlab, with each patch having a signal feeder at the patch's center.
- Integration of a ground plane reflector and substrate beneath the radiating elements.
- Phase shift assignments based on the targeted OAM modes via Eq. (1) for USA, or Eq. (2) for UCA.

- Adaptive meshing using triangular elements by following the EM-field calculation based on MoM.
- Post-processing of radiation patterns and analysis of farfield characteristics.

Third, for evaluating the OAM purity of an antenna array, the following procedures can be executed:

- Establishing high-resolution observation grids at a specified propagation distance.
- EM-field calculation as above-stated, from which phase angle can be computed.
- The quality of phase profile is then assessed. If vortex is observed, continue to the procedures below. Otherwise, the observation size and distance are adjusted to repeat the above, until a vortex wave is obtained.
- The phase profile is sampled with an equal interval over a full circle. For each sample, its *x* and *y* coordinates are calculated and, if needed, rounded to the closest discrete indices.
- Then, DFT is carried out to analyse the phase profile.
- Finally, purity is calculated using Eq. (12).

Let us start comparing the performance of different types of arrays against KPIs, by first examining the feasibility of the arrays for generation of OAM-waves. Specifically, UCA, USA and HCA are examined. The intensity profiles, phase profiles, and elevation patterns of the OAM-beams generated by these arrays are shown in Fig. 7, Fig. 8 and Fig. 9, respectively, when 16 array elements are configured to generate OAM-waves of Mode 1. Explicitly, all the three arrays are capable of producing satisfactory vortex phases with different intensity and phase distributions. For all the three types of arrays, the plots reveal the central hollow, doughnut-shaped intensity profiles. Therefore, it can be confirmed that these arrays are feasible for generating OAM-waves.

Note that, as no GP is employed with HCA, the elevation pattern is symmetric with respect to the azimuth plane passing the origin.

B. COMPARISON OF 16-ELEMENT UCA, USA AND HELICAL ARRAYS GENERATING OAM MODES 2, 3 AND 4

In this subsection, we compare the performance the UCA, USA, HCA and HCSA with 16 array elements, when they are configured to generate OAM-waves of Modes 2-4, respectively.

First, we note that the phase profiles of Mode 1 OAMbeams generated by the 16-element USA, UCA and HCA have already been exhibited in Figs. 7 - 9 in Section IV-A. Now, the phase profiles of the OAM-beams with Modes 2, 3 and 4 generated by the 16-element USA, UCA and HCA are depicted in Fig. 10, Fig. 11 and Fig. 12, respectively. Correspondingly, TABLE 8 quantifies all the phase profiles for OAM-modes 1-4 produced using (10) based on Fig. 7 to Fig. 12. Furthermore, Fig. 13 addresses an example of the 16-element UCA, which demonstrates the spectrum of OAMwaves estimated from (11) and (12). Observe from Fig. 13 that, when UCA is employed to generate an OAM-wave of



Parameters	Frequency	Element Length/Width	Substrate Type	Substrate Thickness	Feed Location	Feed Radius
Value/type	3 GHz	20 mm	Air	1 mm	Center of each patch	1.5mm

TABLE 7: Parameters for antenna arrays.

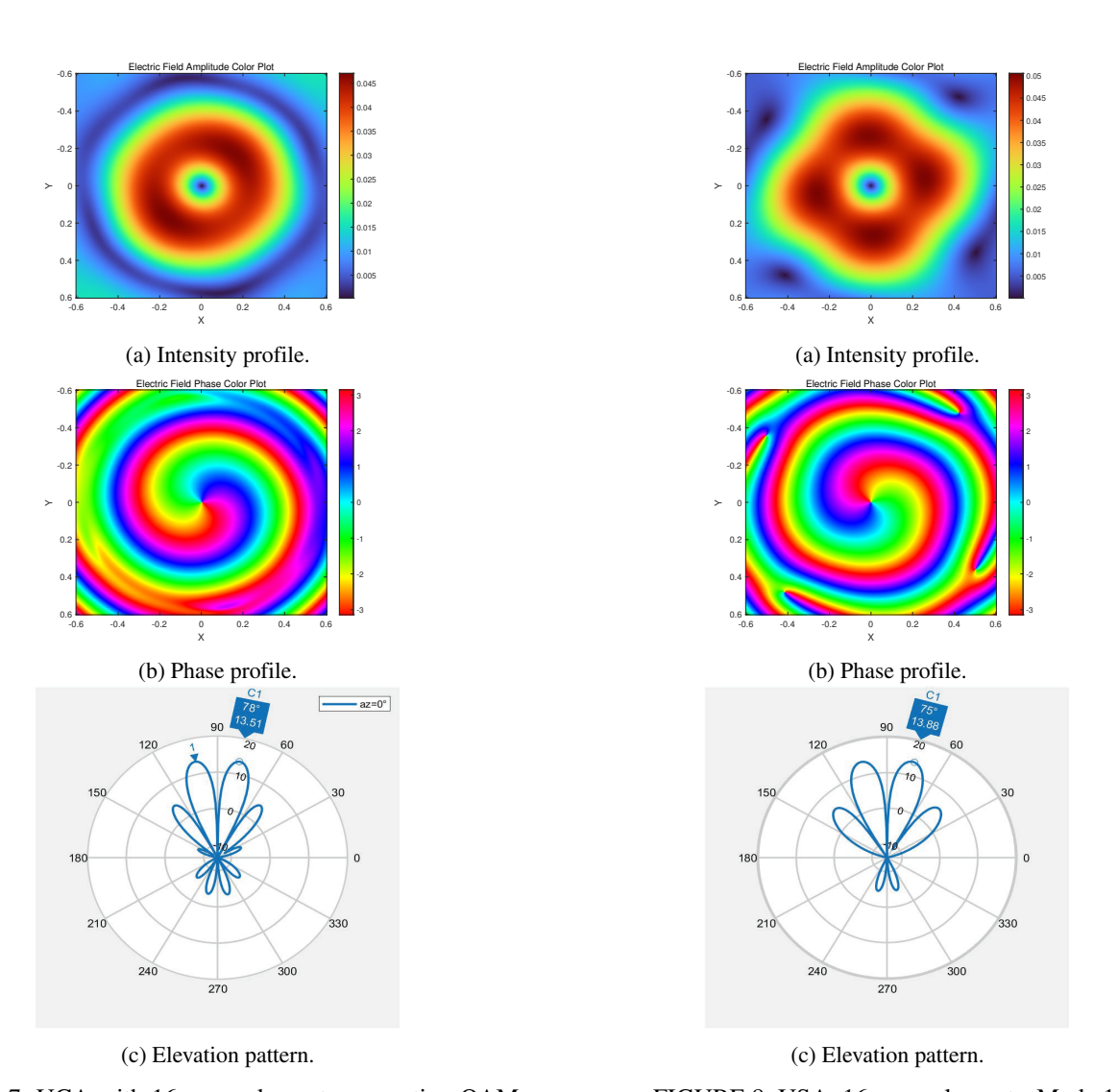


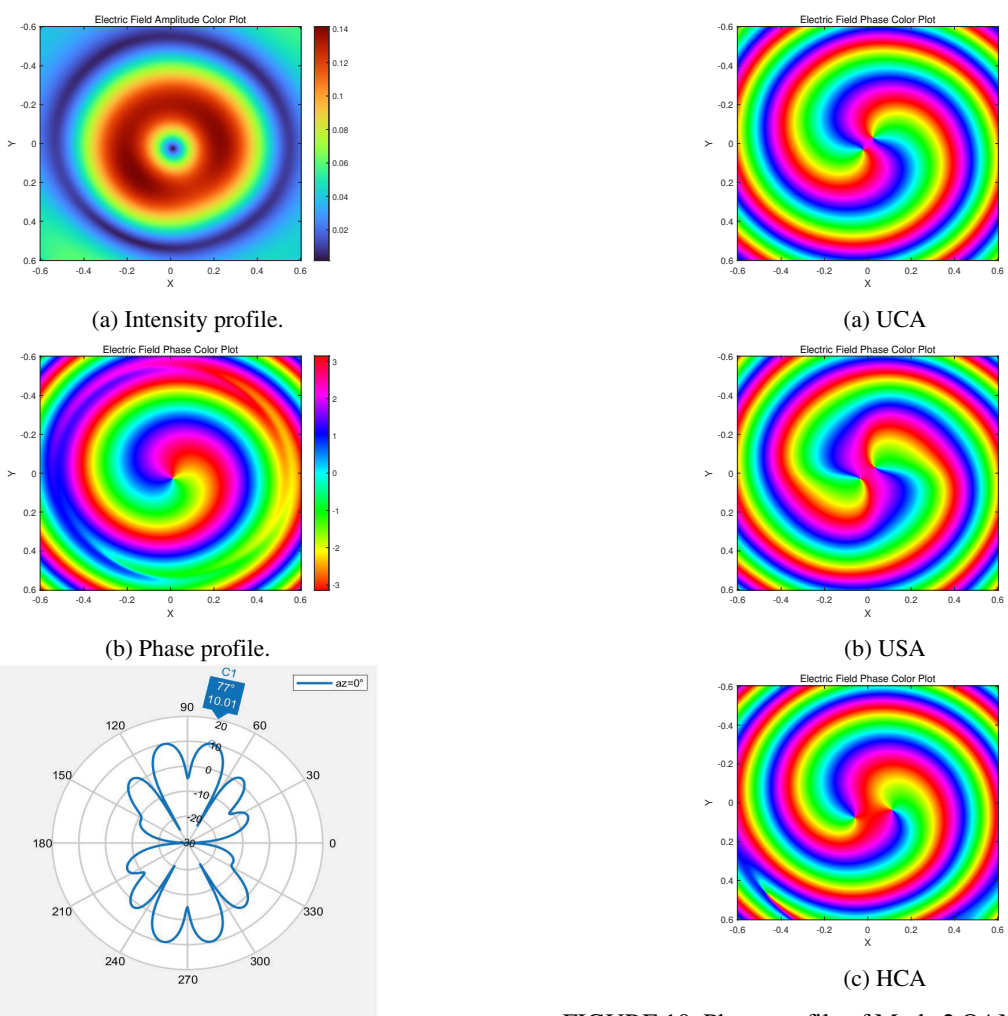
FIGURE 7: UCA with 16 array elements generating OAM-mode 1.

FIGURE 8: USA: 16 array elements, Mode 1.

Mode 1, a peak power of 0.76 pointing to the direction of Mode 1 is available.

From the results shown in Fig. 7 to Fig. 12 and the results provided in TABLE 8, it can be seen that for all considered arrays, there is phase distortion, when Mode 4 OAM-beams are generated. In the context of the smoothness of phase profiles, USA is worse than UCA and HCA, especially in the case of OAM-mode 4. Furthermore, the spirals, the number of which is equal to the OAM-mode number, of USA and UCA are equally spread over the whole 2π azimuth angle. However, the spirals of HCA for OAM-mode 3 or 4 are only distributed within half of the azimuth plane from π to 2π . In contrast, all the considered arrays are capable of generating

the OAM-beams of Modes 1, 2 and 3 with relatively good purity performance. To be more specific, when generating the OAM-beams of low mode, such as Mode 1, 2 or 3, a USA is compatible with UCA and HCA, achieving a similar purity performance. Although it has outstanding directivity in Mode 4, as its data in Table 8 shows, the OAM-beam's purity of USA dramatically degrades, and its vortex phase profile no longer holds, as seen in Fig. 12b. The benefit of using HCA appears, when OAM-beams of Mode 4 are generated. As seen in TABLE 8, HCA is capable of striking a good tradeoff among the three KPIs considered, namely directivity, divergence and purity. However, we should remember that HCA occupies a 3D geometric space, hence behaving poorly in multiplexing applications.



(c) Elevation pattern.
FIGURE 9: HCA: 16 array elements, Mode 1.

FIGURE 10: Phase profile of Mode 2 OAM-beams generated by the 16-element UCA, USA and HCA, respectively.

As seen in TABLE 8, the directivity of the OAM-beams generated by UCA degrades significantly, when relatively high modes are transmitted, as seen in the 2nd row. Moreover, the effect of GP on the directivity of UCA is significant, when comparing the directivity values in the 2nd and 4th rows in TABLE 8. By contrast, when comparing the divergence angles, as seen in Rows 2 and 4 in TABLE 8, the effect of GP is ignorable. Additionally, when comparing UCA and HCA, it reveals that UCA outperforms HCA in terms of directivity, divergence and purity, when OAM-modes of 1, 2, and 3 are considered. By contrast, for OAM-mode 4, UCA is outperformed by HCA for all the three KPIs.

The elevation patterns of the Mode 4 OAM-beams generated by the 16-element USA and HCA are shown in Fig. 14. As seen in Fig. 14a, the beam by USA is not hollow any more but, instead, has a central beam only slightly weaker than the main beam of Mode 4. Hence, USA with 16 array elements is not suitable for generating the OAM-beams with modes higher than 3. This implies that the 'good' directivity of the

Mode 4 OAM-beam by USA, as shown in TABLE 8, has no practical meaning. As seen in Fig. 14b, although the central null does not exist, the HCA may still be useful for generating the Mode 4 OAM-beams, as the result that the central beam is more than 10 dB below the main OAM-beam of Mode 4.

The phase profiles for the OAM-beams of Modes 2 and 4 generated by HCSA are depicted in Fig. 15a and Fig. 15b, respectively. By comparing these profiles with that demonstrated in Fig. 10a, Fig. 12a and Fig. 15, it can be seen that, unlike HCA, the phase profiles of the OAM-beams by HCSA are close to that of the OAM-beams by UCA, all showing clear spirals.

Correspondingly, the comparison of directivity, divergence angle, and purity between the OAM-beams by HCA and HCSA is provided in TABLE 9. Explicitly, for both OAM-modes 2 and 4, HCA is capable of yielding better directivity than HCSA. By contrast, both arrays generate the Mode 2 or 4 OAM-beams with nearly the same divergence and purity performance, although it seems that the purity of OAM-beam by HCSA decreases slightly faster than that of the OAM-

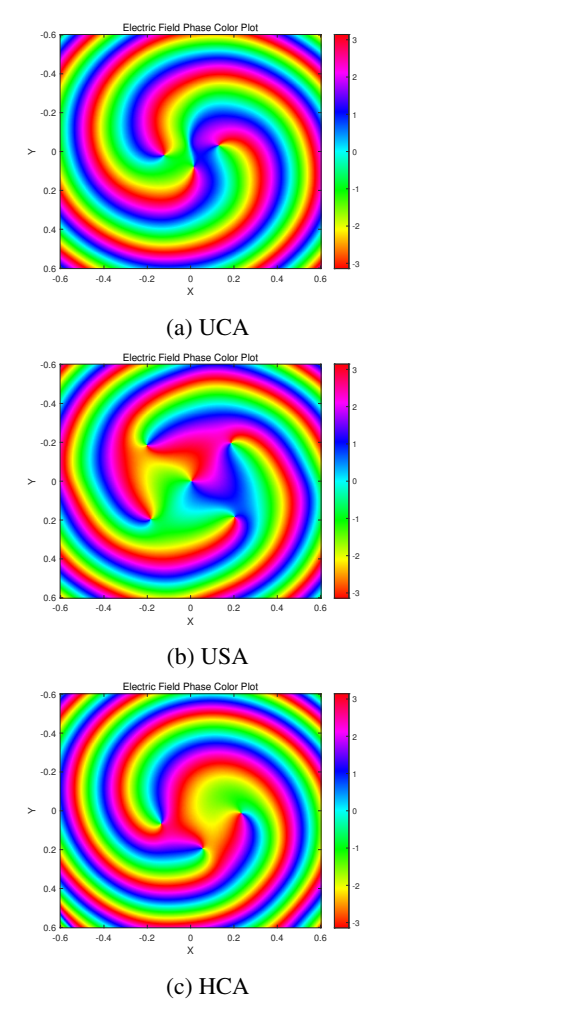


FIGURE 11: Phase profile of Mode 3 OAM-beams generated by 16-element UCA, USA and HCA, respectively.

beam by HCA, when OAM-mode is increased from 2 to 4. Note that, as 16 is not divisible by 3, this makes HCSA infeasible for generating the Mode 3 OAM-beams. Hence, OAM-mode 3 is not considered in TABLE 9.

The directivity, divergence angle, and purity of OAM-waves generated by the different antenna arrays of 16 elements operated at 30 GHz mmWave bands are compared in Table 10. When comparing Table 8 with Table 10, we can observe that, in most cases, the performance yielded in higher frequency reveals only subtle difference from the corresponding one achieved at lower frequency, which typically falls within the margin of simulation and rounding errors. However, in comparison with Table 8, the purity of USA operated at 30 GHz degrades for all modes, with mode 4 the severest, indicating that USA is not suitable for high-frequency applications.

C. COMPARISON OF 8- OR 12-ELEMENT UCA AND USA

In this subsection, we compare the performance of USA and UCA, when their numbers of array elements are relatively

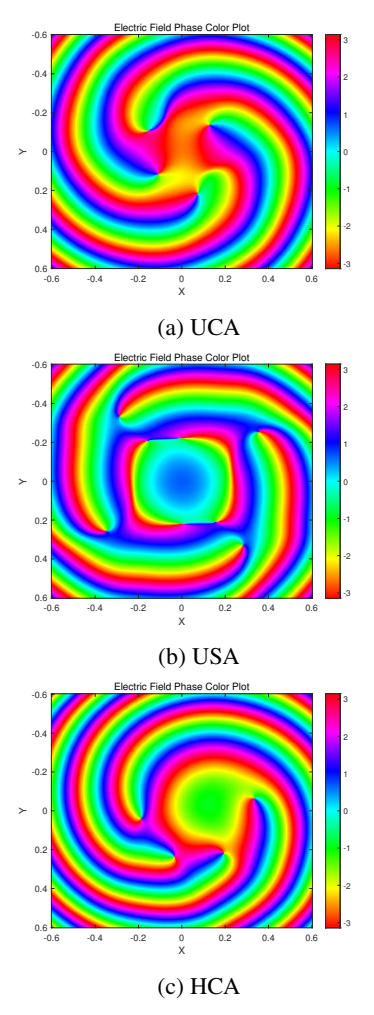


FIGURE 12: Phase profile of Mode 4 OAM-beams generated by 16-element UCA, USA and HCA, respectively.

small, namely 8 elements in TABLE 11 and 12 in TABLE 12. As seen in the two tables, there are some values missing, which is because the arrays with such numbers of elements are infeasible for or incapable of generating the OAM-beams of such modes. Also seen in TABLE 11, there are two values for directivity and two values for divergence angle associated with the OAM-mode 2 of USA.

The results in TABLE 11 show that, with the previous parameter settings and the definition in Section III-B, the UCA with 8 array elements is capable of generating the OAM-beams of 3 different modes, namely Modes 1, 2, 3. However, it is infeasible for generating an OAM-beam of Mode 4, due to the poor purity performance of 0.15, which causes an abnormal directivity of 8.05. By contrast, the 8-element USA is only feasible for generating the OAM-beams of Mode 1 or 2. When comparing the 8-element USA and UCA, we conclude that UCA outperforms USA in terms of all the three KPIs.

Similar observations can be obtained from TABLE 12 considering the 12-element UCA and USA. In general, when

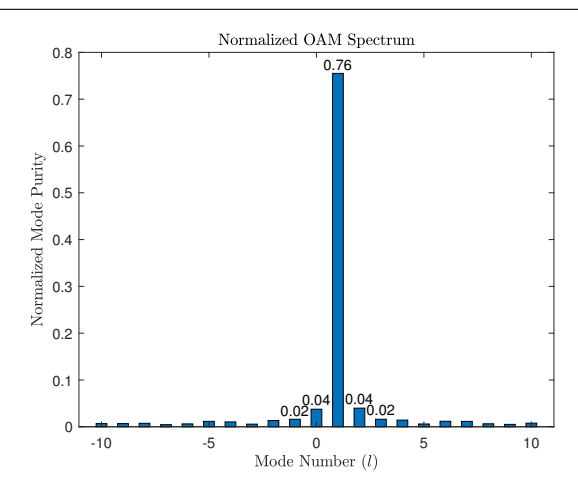


FIGURE 13: Purity spectrum of OAM-waves generated by a UCA with 16 elements.

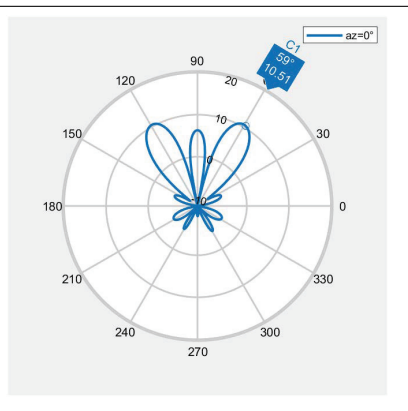
Directivity (dBi)	Mode 1	Mode 2	Mode 3	Mode 4
USA	13.88	8.93	6.45	10.51
UCA	13.51	12.1	10.19	5.71
HCA	10.01	8.61	6.15	8.13
UCA (No GP)	9.62	7.74	6.19	5.47
Divergence Angle (°)	Mode 1	Mode 2	Mode 3	Mode 4
USA	15	24	20	31
UCA	12	20	28	36
HCA	13	22	29	33
UCA (No GP)	12	21	29	38
Purity	Mode 1	Mode 2	Mode 3	Mode 4
USA	0.68	0.54	0.5	0.43
UCA	0.76	0.62	0.5	0.43
HCA	0.71	0.57	0.5	0.44

TABLE 8: Comparison of directivity, divergence angle and purity of OAM-waves generated by 16-element arrays operated at 3 GHz.

Modes 1-3 are considered, UCA outperforms USA in terms of all the three KPIs, except that the divergence angle of the Mode 3 OAM-beam by UCA is 37^{o} , which is larger than that of the Mode 3 OAM-beam by USA, which is 26^{o} . Note that, similar to the result shown in TABLE 8, as shown in TABLE 12, the directivity of the Mode 4 OAM-beam by USA gives a relatively big value. This is because of the significant reduction in purity and the disappearance of the central null, as seen in Fig. 14a for the 16-element USA, resulting in the deteriorated vortex properties.

In summary, from the demonstrations and results in Section IV-A to Section IV-C, we have the following observations:

- For all the arrays considered, increasing the number of array elements enables to improve directivity and increase the number of potentially producible modes.
- When the vortexes corresponding to two OAM-modes are not severely distorted, in general, the divergence angle of the OAM-beam with a smaller mode number is smaller than that of the OAM-beam with a bigger mode number.
- If the phase profiles are severely distorted, resulting in



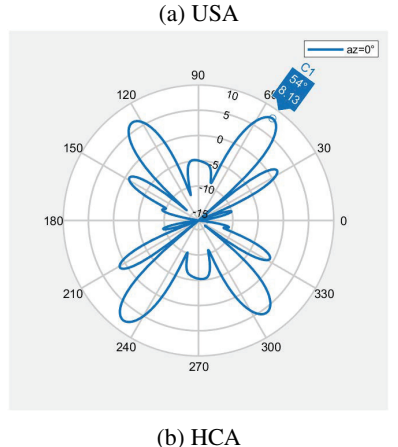


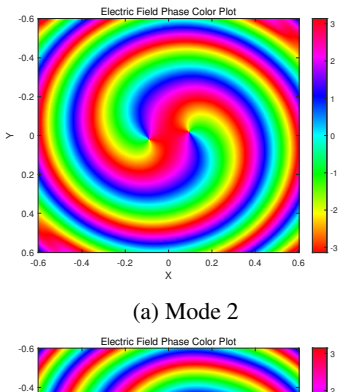
FIGURE 14: Elevation patterns of 16-element USA and HCA generating OAM-beams of Mode 4.

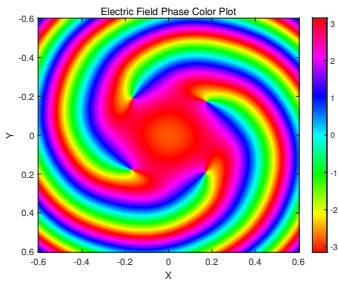
Directivity (dBi)	Mode 2	Mode 4
HCA	8.61	8.13
HCSA	7.95	5.26
Divergence Angle (°)	Mode 2	Mode 4
HCA	22	36
HCSA	21	36
Purity	Mode 2	Mode 4
HCA	0.57	0.44
HCSA	0.61	0.4

TABLE 9: Comparison of directivity, divergence angle and purity of OAM-waves generated by HCA and HCSA.

the loss of the vortex property, the divergence angle and directivity of OAM-beams become abnormal and their values are invalid.

- The purity performance of OAM-beams by UCA is always better than or at least similar to that of OAMbeams by USA. The purity performance of OAM-beams by USA degrades significantly as the mode number increases.
- Specifically, when the arrays with 12 and 16 array elements are respectively used to transmit OAM-beams of Mode 1, the OAM-beams by USA shows slightly better directivity than that by UCA. Again, the directivity of OAM-beams by USA degrades significantly, as the OAM-mode number increases to 2, 3, etc., thus,





(b) Mode 4

FIGURE 15: Phase profiles of 16-element HCSA.

Directivity (dBi)	Mode 1	Mode 2	Mode 3	Mode 4
USA	13.58	9.09	6.17	10.77
UCA	13.78	11.66	9.72	7.8
HCA	9.96	8.51	6.07	8.02
HCSA	/	7.9	/	5.3
Divergence Angle (°)	Mode 1	Mode 2	Mode 3	Mode 4
USA	14	24	21	30
UCA	13	21	29	35
HCA	14	22	29	36
HCSA	/	21	/	37
Purity	Mode 1	Mode 2	Mode 3	Mode 4
USA	0.64	0.51	0.43	0.14
UCA	0.75	0.61	0.5	0.43
HCA	0.71	0.57	0.5	0.43
HCSA	/	0.61	/	0.4

TABLE 10: Comparison of directivity, divergence angle, and purity of OAM-waves generated by 16-element arrays operated at 30 GHz.

making USA less feasible for operation with relatively high OAM-modes.

 Overall, in comparison with the other types of arrays considered, UCA enables space saving, relatively small divergence angle, moderate to good directivity, and relatively high purity. Hence, it is capable of striking a best trade-off for practical applications, which may explain why UCA has mainly been invoked in the published research works.

So far, different arrays have been compared when OAM-modes 1-4 are considered. In the next subsection, we explore the feasibility of some arrays for generating the OAM-beams with the OAM-mode number higher than 4, namely, Modes 5 and 6.

Directivity (dBi)	Mode 1	Mode 2	Mode 3	Mode 4
USA	7.92	4.83 & 3.31	0.28	/
UCA	9.7	7.66	2.74	8.05
Divergence Angle (°)	Mode 1	Mode 2	Mode 3	Mode 4
USA	23	40 & 43	/	/
UCA	22	39	40	45
Purity	Mode 1	Mode 2	Mode 3	Mode 4
USA	0.73	0.55	/	/
UCA	0.74	0.59	0.46	0.15

TABLE 11: Directivity, divergence angle and purity of OAM-waves generated by 8-element USA and UCA.

Directivity (dBi)	Mode 1	Mode 2	Mode 3	Mode 4
USA	12.67	7.63	3.84	7.83
UCA	12.09	10.34	8.16	6.27
Divergence Angle (°)	Mode 1	Mode 2	Mode 3	Mode 4
USA	19	31	26	/
UCA	17	27	37	44
Purity	Mode 1	Mode 2	Mode 3	Mode 4
USA	0.74	0.52	0.32	0.12
UCA	0.74	0.61	0.47	0.29

TABLE 12: Directivity, divergence angle and purity of OAM-waves generated by 12-element USA and UCA.

D. PERFORMANCE AT HIGHER OAM-MODE AND PURITY ELEVATION IMPROVEMENT

No. of Array	U	CA	USA		
Elements	Mode 5	Mode 6	Mode 5	Mode 6	
10	0.05	/	/	/	
11	0.25	/	/	/	
12	0.38	0.14	0.18	0.03	
14	0.37	0.33	/	/	
16	0.38	0.33	0.32	0.17	
24	0.38	0.33	0.32	0.19	

TABLE 13: Purity versus the number of array elements of Modes 5 and 6 OAM-beams generated by UCA and USA.

The results of the different antenna arrays for OAM-modes 1-4, as shown in TABLE 11, demonstrate that it is difficult for an 8-element array to generate Mode 4 OAM-beams having the practically meaningful purity, even when UCA is employed. To further investigate the performance of LPM and purity of OAM-beams by UCA and USA, we consider the UCA and USA with various number of array elements to generate the OAM-beams of Modes 5 and 6. The purity performance results are shown in TABLE 13. Note that, as a USA cannot be built with 14 array elements, there are no purity results in this case for USA. Furthermore, due to the rounding error in calculation, the purity of Mode 5 OAM-beams by UCA with 14 array elements is 0.37, slightly lower than the other value of 0.38 for the cases of 12, 16 and 24 array elements.

From the results of TABLE 13 we can observe that a 10-element UCA is unable to generate a satisfactory OAM-beam of Mode 5, while an 11-element UCA is capable of. Hence, the results follow the relationship of $-N/2+1 \le l_{\rm max} \le N/2-1$ [8, 49, 72, 94]. As the results in the Table show, the purity of the OAM-beams by an 11-element UCA is much

IEEE Access

higher than that of the OAM-beams by a 10-element UCA. When the number of array elements is increased to 12, the purity performance reaches about 0.38, and any further increasing the number of array elements does not improve purity. Similar purity performance tendency can also be observed with the Mode 6 OAM-beams generated by UCAs, except that UCAs with more than 12 array elements are required to attain satisfactory purity performance. By contrast, for USAs, while their generated OAM-beams share similar performance tendency as that by UCAs, the purity performance of OAM-beams generated by USAs is always poorer than that of OAM-beams generated by the corresponding UCAs.

As shown in TABLE 13, when 21 uniform samples from $[-\pi,\pi]$ are considered, the purity saturates at a value, which does not improve when further increasing the number of array elements. This is the consequence of the limited number of samples in $[-\pi,\pi]$ used to evaluate the purity by (11) and (12). The purity may be improved, when more samples are used. To illustrate this, we increase the number of samples in $[-\pi,\pi]$ to 41 to estimate the purity performance, when OAM-beams of Modes 1, 5 and 6 are generated by UCAs with different number of array elements. The results are compared with the previous ones estimated from 21 samples, which are shown in TABLE 14.

As shown in TABLE 14, increasing the number of sampling points in $[-\pi, \pi]$ improves the purity. However, it is implied that the achievable purity is determined by both the number of samples in $[-\pi, \pi]$ and the number of elements of antenna array. Specifically when Mode 1 is considered, given the number of array elements being 8 or 12, employing 41 samples instead of 21 introduces little purity improvement. By contrast, when the number of array elements is 16, 20 or 24, the purity improvement is apparent. Furthermore, it appears that purity becomes saturated against both the number of array elements and the number of samples in $[-\pi, \pi]$. As seen in TABLE 14, given N = 21 or 41 for Mode 1, the purity converges to a fixed value when increasing the number of array elements. On the other hand, given 8 or 12 array elements, the purity is also nearly fixed, when the number of samples is increased from 21 to 41. The purity saturation in this second case is further explained in Fig. 16, where a UCA with 16 elements is considered. When ignoring the fluctuation from simulations, Fig. 16 shows that for a given OAM-mode, the purity converges to a value, when the number of samples in $[-\pi, \pi]$ becomes sufficiently high. Additionally, Fig. 16 explicitly shows that the purity of OAM-waves decreases as the array is configured to generate an OAM-beam of higher mode. Finally, as shown in TABLE 14, the purity improvement to the high OAM-mode 5 or 6 is more significant than that to the OAM-mode 1, as the number of samples in $[-\pi, \pi]$ is increased from 21 to 41.

E. PERFORMANCE OF CONCENTRIC UNIFORM CIRCULAR ARRAYS

In this subsection, the KPIs of CUCA with two rings are demonstrated and analyzed. To evaluate the KPIs, the two

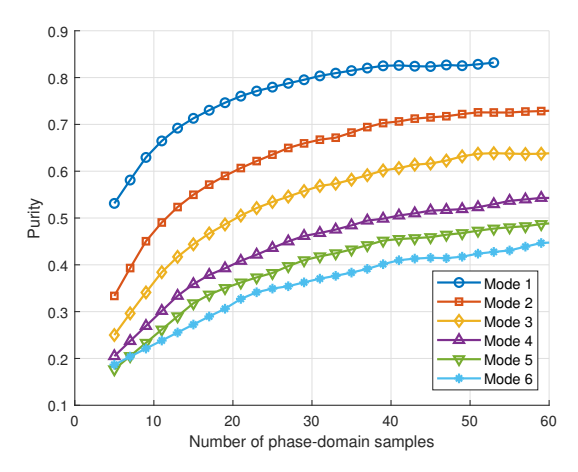


FIGURE 16: Illustration of purity convergence, when increasing the number of uniformly sampled points in $[-\pi, \pi]$ of the phase profile of the UCA with 16 array elements.

UCAs of CUCA are set as follows. We assume that the CUCA has the arrangement of array elements as shown in Fig. 4. Both rings have the same number of elements; the radius of the outer ring is twice of that of the inner ring and the elements of the outer ring are aligned in a straight line from the ring center with the elements on the inner ring. The two UCAs are set to jointly produce two OAM-modes, namely Modes 1 and 2, or Modes 2 and 3. The total purity is normalised to 1, implying that two perfect OAM-beams will both have the purity of 0.5.

As an example, considering the 16-elements CUCA generating the OAM-beams of Modes 1 and 2, the purity spectrum is shown in Fig. 17. This spectrum explains that although CUCA is capable of jointly generating OAM-beams of multiple modes, the leakage between different mode OAM-beams is severer compared to that of the OAM-beams of different OAM-modes generated by separate UCAs, which has the spectrum as shown in Fig. 13. Specifically, as shown in TABLE 8, the purities of OAM-beams of Modes 1 and 2 generated by two separate UCAs are 0.76 and 0.62, respectively. By contrast, the purities of the OAM-beams of the same Modes 1 and 2 jointly generated by CUCA are $2 \times 0.35 = 0.7$ and $2 \times 0.21 = 0.42$, respectively. Note that here a factor of 2 is applied because the total purity in Fig. 17 is normalized to 1.

When comparing the results in TABLE 8, TABLE 11 and TABLE 15, it can be seen that the directivity and divergence performance of a CUCA are, respectively, better than that of a UCA, if the number of elements per ring of the CUCA is the same as that of the UCA. However, in the case that the total number of elements of a CUCA is the same as that of a UCA, then, when the CUCA jointly generates the OAM-beams of multiple modes while the UCA only generates an OAM-beam of one mode, the UCA outperforms the CUCA in terms of both the directivity and divergence performance. Even though the number of array elements per ring of a CUCA is the same as that of a UCA, the purity of the OAM-beams

No. of Array	Mode 1		Mode 5		Mode 6	
Elements	N = 21	N = 41	N = 21	N = 41	N = 21	N = 41
8-element	0.74	0.75	/	/	/	/
12-element	0.74	0.75	0.38	0.41	/	/
16-element	0.76	0.78	0.38	0.48	0.33	0.41
20-element	0.77	0.83	/	/	/	/
24-element	0.77	0.83	0.38	0.51	0.33	0.45

TABLE 14: Purity versus the number of array elements of Modes 1, 5 and 6 OAM-beams generated by UCAs, when N=21 or 41 samples uniformly from $[-\pi,\pi]$ are used to compute purity.

Modes	No. of Elements per Ring	Divergence Angle	Directivity	Purity
1, 2	8	22	10.04	0.35, 0.1
1, 2	16	11	14.82	0.35, 0.21
2, 3	16	17	12.45	0.29, 0.23

TABLE 15: Performance of OAM-beams generated by the CUCA with two rings of sub-arrays.

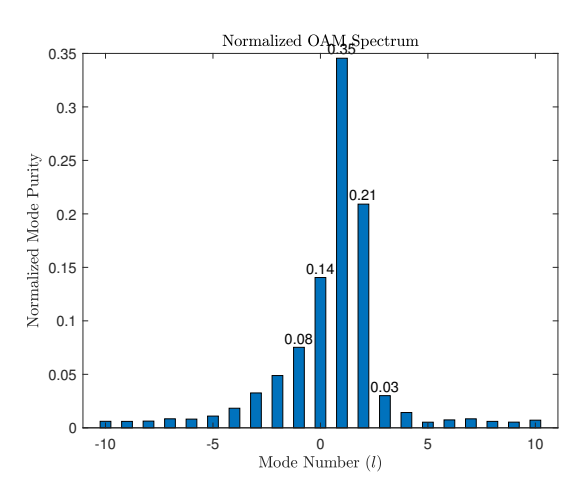


FIGURE 17: Purity spectrum of OAM-beams generated by CUCA with two rings of sub-arrays, each having 16 array elements, where two rings of sub-arrays jointly generate two OAM-beams of Modes 1 (inner ring) and 2 (outer ring).

jointly generated by the CUCA is worse than that separately generated by the UCAs. Additionally, as demonstrated in the third row (corresponding to Modes 1 and 2) and fourth row (corresponding to Modes 2 and 3) in TABLE 15, both the directivity and convergence performance become worse, when the same CUCA with 16 array elements is employed to generate the higher OAM-modes of 2 and 3, instead of the OAM-modes of 1 and 2.

V. CONCLUDING SUMMARY AND FURTHER RESEARCH ISSUES

A. CONCLUDING SUMMARY

The motivation of this paper is to provide a comprehensive comparison of the typical antenna arrays studied for OAM-wave generation, including USA, UCA, HCA, HCSA and CUCA, so as to gain knowledge about the design and performance of the OAM-assisted wireless systems. For the objective, the unified KPIs, including directivity, LPM, OAM-mode multiplexing capability, divergence angle, and purity, were first described, based on which the considered antenna

arrays were compared from different perspectives. From the studies, general conclusions derived include the followings.

The number of array elements imposes a big impact on the qualities of the OAM-beams the arrays generate. When the number of array elements is sufficient, all considered arrays are capable of generating high-quality OAM-beams of relatively low modes, such as Mode 1 or 2. Given the number of array elements, generating an OAM-beam carrying a relatively high mode, such as Mode 5 or 6, with certain purity requirement becomes challenging. In general, simultaneously generating the beams by one array to multiplex multiple OAM-modes with purity requirements is highly challenging. Specifically, when employing CUCA, the multimode OAM-beams with each separately generated by one sub-UCA presents higher purity than the corresponding ones jointly generated by a CUCA.

Due to the propagation's divergent behaviours of the OAMbeams carrying different modes, the receiving of OAM multiplexing signals is highly demanding. To achieve similar detection performance of the information carried by different OAM-modes, transmitter must be designed carefully, so that the OAM-beams carrying different modes can be focused on one receive ring-array for the best possible sampling quality. Otherwise, multiple receive ring-arrays of different sizes should be utilized, with each matching to one of the transmitted OAM-modes. Moreover, due to the divergence property of OAM-beams, the performance of OAM-based communications may be very sensitive to transmission distance. Without transmitter reconfiguration, a fixed-size receive array is only optimum at one distance from transmitter, moving away from or close to transmitter may result in significant performance degradation.

Each type of arrays presents its unique trade-off with respect to achievable performance and implementation challenges. For example, while HCA and HCSA can generate OAM-waves without relying on PSNs, they are infeasible for reconfiguration and the implementation of MDM. Overall, when taking into account both performance and implementation flexibility, UCA, especially its generalized CUCA, constitutes the best choice, which explains why most existing studies considered UCA by default, although significant fur-

ther research on CUCA is needed for a deep understanding of its implementation, application opportunities and achievable performance.

B. FURTHER RESEARCH IDEAS

Based on our studies, some further research issues on OAM can be identified, which are listed as follows.

- Array design: High-efficiency and high-flexibility arrays feasible for reconfiguration are crucial for OAMassisted systems to operate and attain good performance. Research issues on the design of OAM-generating arrays include but not limited to the followings. First, there are various types, including phased arrays, reflectarrays, transmitarrays, etc., to consider for designing OAMgenerating arrays. The choices of array type and design also need to consider the application scenarios. Second, OAM-generating arrays having low divergence angle and good beam-focusing capability are required to extend communication coverage. Third, OAM can be beneficial to near-field, far-field, intra-chip and interchip communications. Furthermore, OAM-waves may propagate in the media other than air, such as semiconductor, in intra-chip communications. Accordingly, researches are required to design the OAM-generating arrays that are suitable for these application scenarios. Additionally, the arrays for transmitting OAM-waves in different frequency bands, such as, sub-6 GHz band, millimetre wave (mmWave) band and THz band, respectively, are required.
- Transmitter processing: While the physically well-structured arrays may achieve good beam focusing over certain transmission range, transmitter processing may further enhance the focusing capability over larger propagation ranges. Furthermore, with transmitter processing, the conventional preprocessing techniques, such as sub-channel allocation, water-filling based power-allocation, etc., richly developed with MIMO may be employed to improve the performance of OAM-assisted wireless systems.
- Receiver processing: First, design of the receive arrays robust to transmission distance is highly important. Similarly, it is desirable that receive arrays can adapt to the divergence of OAM-waves. Once OAM-carrying signals are obtained, the receiver processing would be conventional, with the objectives, such as, to maximize signal to-interference-plus-noise ratio (SINR), minimize various types of interference, including inter-mode interference, co-channel interference, etc.
- Positioning: OAM-beam focusing and some other transmitter processing implementation need knowledge of receiver's position, orientation, or even the positions of individual elements on receive array [159], to execute optimization. Hence, the positioning methods and algorithms capable of providing high accuracy positioning are needed. Furthermore, when integrated sensing and communication (ISAC) is considered in OAM-assisted

- system, there are numerous challenges to meet, while simultaneously having a variety of opportunities for system design and optimization.
- Multi-user OAM-assisted systems: Existing researches on OAM have focused dominantly on point-to-point communications. Without any doubt, the extension to multi-user scenarios has a lot of challenges to meet, requesting great effort for the related research issues.
- Effect of mobility: Performance of the OAM-assisted wireless systems is sensitive to mobility [160–162]. System reconfiguration and optimization depend on the location information of the involved communication terminals. Hence, the mobilities of communication terminals impose a big impact on the design and performance of the OAM-assisted wireless systems. Accordingly, methods for accurate prediction of mobilities and efficient usage of mobility information are critical, which are also highly challenging for design and practical implementation.
- **Resource allocation**: In an OAM-assisted wireless system, there are extra resources provided by multiple OAM-modes, in addition to the conventional resources from time, frequency and space domains. While this has the potential for a higher throughput, it also makes resource allocation more challenging. Hence, low-complexity high-efficiency resource-allocation algorithms for various types of OAM-assisted wireless networks are expected to be developed.
- Integration of OAM with other 6G techniques: In addition to OAM, currently, there are a range of advanced technologies being studied for 6G applications, including mmWave and THz, orthogonal time-frequency-space (OTFS) and affine frequency division multiplexing (AFDM), reconfigurable intelligent surface (RIS), ultra-massive and holographic MIMO, etc. Generally, OAM may be integrated with any of these technologies to provide extra degrees of freedom. However, great research effort is needed to reveal the extra contribution possibly made by the employment of OAM.

REFERENCES

- M. H. Alsharif, et al., "Milestones of wireless communication networks and technology prospect of next generation (6G)." Computers, Materials & Continua, vol. 71, no. 3, 2022.
- [2] K. G. Eze, M. N. Sadiku, and S. M. Musa, "5G wireless technology: A primer," *International journal of scientific engineering and technology*, vol. 7, no. 7, pp. 62–64, 2018.
- [3] W. Cheng, W. Zhang, H. Jing, S. Gao, and H. Zhang, "Orbital angular momentum for wireless communications," *IEEE Wireless Communications*, vol. 26, no. 1, pp. 100–107, 2018.
- [4] 2015. [Online]. Available: https://www.itu.int/dms_pub/itu-r/opb/rep/R-REP-M.2370-2015-PDF-E.pdf
- Z. Wei, et al., "Evolution of optical wireless communication for B5G/6G," Progress in Quantum Electronics, vol. 83, p. 100398, 2022.
 [Online]. Available: https://www.sciencedirect.com/science/article/pii/ S0079672722000246
- [6] S. K. Noor, M. N. M. Yasin, A. M. Ismail, M. N. Osman, P. J. Soh, N. Ramli, and A. H. Rambe, "A review of orbital angular momentum vortex waves for the next generation wireless communications," *IEEE Access*, vol. 10, pp. 89 465–89 484, 2022.

- [7] L. Allen, M. W. Beijersbergen, R. Spreeuw, and J. Woerdman, "Orbital angular momentum of light and the transformation of laguerre-gaussian laser modes," *Physical review A*, vol. 45, no. 11, p. 8185, 1992.
- [8] B. Thide, et al., "Utilization of photon orbital angular momentum in the low-frequency radio domain," *Physical review letters*, vol. 99, no. 8, p. 087701, 2007.
- [9] F. Tamburini, et al., "Encoding many channels on the same frequency through radio vorticity: first experimental test," New journal of physics, vol. 14, no. 3, p. 033001, 2012.
- [10] C. Guo, et al., "An OAM patch antenna design and its array for higher order OAM mode generation," *IEEE Antennas and Wireless Propagation* Letters, vol. 18, no. 5, pp. 816–820, 2019.
- [11] F. Qin, et al., "A four-mode OAM antenna array with equal divergence angle," *IEEE Antennas and Wireless Propagation Letters*, vol. 18, no. 9, pp. 1941–1945, 2019.
- [12] N. Kou and S. Yu, "Low sidelobe orbital angular momentum vortex beams based on modified bayliss synthesis method for circular array," *IEEE Antennas and Wireless Propagation Letters*, vol. 21, no. 5, pp. 968– 972, 2022.
- [13] F. Mao, et al., "Massive OAM-MIMO transmission scheme for 5G networks and beyond," IET Communications, vol. 15, no. 7, pp. 973–979, 2021.
- [14] H. Jing, W. Cheng, Z. Li, and H. Zhang, "Concentric UCAs based low-order OAM for high capacity in radio vortex wireless communications," *Journal of Communications and Information Networks*, vol. 3, no. 4, pp. 85–100, 2018.
- [15] C. Zhou, et al., "Capacity and security analysis of multi-mode orbital angular momentum communications," *IEEE Access*, vol. 8, pp. 150 955– 150 963, 2020.
- [16] L. Wang, X. Ge, R. Zi, and C.-X. Wang, "Capacity analysis of orbital angular momentum wireless channels," *IEEE Access*, vol. 5, pp. 23 069– 23 077, 2017.
- [17] A. Z. Ilic, et al., "Optimized planar printed UCA configurations for OAM waves and the associated OAM mode content at the receiver," *International Journal of Communication Systems*, vol. 36, no. 18, p. e5623, 2023.
- [18] D. Lee, et al., "Orbital angular momentum (OAM) multiplexing: An enabler of a new era of wireless communications," *IEICE Transactions* on Communications, vol. E100.B, no. 7, pp. 1044–1063, 2017.
- [19] T. Yuan, Y. Cheng, H. Wang, and Y. Qin, "Mode characteristics of vortical radio wave generated by circular phased array: Theoretical and experimental results," *IEEE Transactions on Antennas and Propagation*, vol. 65, no. 2, pp. 688–695, 2017.
- [20] Y. B. Dhanade, et al., "Mode purity analysis of an orbital angular momentum antenna," in 2022 IEEE Microwaves, Antennas, and Propagation Conference (MAPCON). IEEE, 2022, Conference Proceedings, pp. 1341–1345.
- [21] J. Ma, et al., "Research on the purity of orbital angular momentum beam generated by imperfect uniform circular array," *IEEE Antennas and Wireless Propagation Letters*, vol. 20, no. 6, pp. 968–972, 2021.
- [22] Y. Huang, et al., "Generation of broadband high-purity dual-mode OAM beams using a four-feed patch antenna: theory and implementation," Scientific reports, vol. 9, no. 1, p. 12977, 2019.
- [23] X. Xiong, H. Lou, and X. Ge, "Modeling and optimization of OAM-MIMO communication systems with unaligned antennas," *IEEE Transactions on Communications*, vol. 70, no. 6, pp. 3682–3694, 2022.
- [24] Z. Zhang, et al., "The capacity gain of orbital angular momentum based multiple-input-multiple-output system," *Scientific reports*, vol. 6, no. 1, p. 25418, 2016.
- [25] T. M. Olaleye, P. A. Ribeiro, and M. Raposo, "Generation of photon orbital angular momentum and its application in space division multiplexing," *Photonics*, vol. 10, no. 6, p. 664, 2023. [Online]. Available: https://www.mdpi.com/2304-6732/10/6/664
- [26] H. Zhang, et al., "A hybrid cladding ring-core photonic crystal fibers for OAM transmission with weak spin-orbit coupling and strong bending resistance," *Photonics*, vol. 10, no. 4, p. 352, 2023. [Online]. Available: https://www.mdpi.com/2304-6732/10/4/352
- [27] T. Hu, et al., "OFDM-OAM modulation for future wireless communications," *IEEE Access*, vol. 7, pp. 59 114–59 125, 2019.
- [28] E.-M. Amhoud, M. Chafii, A. Nimr, and G. Fettweis, "OFDM with index modulation in orbital angular momentum multiplexed free space optical links," in 2021 IEEE 93rd Vehicular Technology Conference (VTC2021-Spring). IEEE, 2021, Conference Proceedings, pp. 1–5.

- [29] R. Chen, W. Yang, H. Xu, and J. Li, "A 2-D FFT-based transceiver architecture for OAM-OFDM systems with UCA antennas," *IEEE Trans*actions on Vehicular Technology, vol. 67, no. 6, pp. 5481–5485, 2018.
- [30] L. Liang, W. Cheng, W. Zhang, and H. Zhang, "Mode hopping for antijamming in radio vortex wireless communications," *IEEE Transactions* on Vehicular Technology, vol. 67, no. 8, pp. 7018–7032, 2018.
- [31] X. Dong, S. Zhao, and B. Zheng, "A quantum multiple access communications scheme using orbital angular momentum," *Journal* of Electronics (China), vol. 30, no. 2, pp. 145–151, 2013. [Online]. Available: https://doi.org/10.1007/s11767-013-3009-2
- [32] A. Al Amin and S. Y. Shin, "Channel capacity analysis of non-orthogonal multiple access with OAM-MIMO system," *IEEE Wireless Communica*tions Letters, vol. 9, no. 9, pp. 1481–1485, 2020.
- [33] E. Basar, "Orbital angular momentum with index modulation," *IEEE Transactions on Wireless Communications*, vol. 17, no. 3, pp. 2029–2037, 2018
- [34] M. Z. Chowdhury, M. Shahjalal, S. Ahmed, and Y. M. Jang, "6G wire-less communication systems: Applications, requirements, technologies, challenges, and research directions," *IEEE Open Journal of the Communications Society*, vol. 1, pp. 957–975, 2020.
- [35] H. Yang, et al., "A THz-OAM wireless communication system based on transmissive metasurface," *IEEE Transactions on Antennas and Propa*gation, vol. 71, no. 5, pp. 4194–4203, 2023.
- [36] R. Chen, et al., "Multi-User Orbital Angular Momentum Based Terahertz Communications," *IEEE Transactions on Wireless Communica*tions, vol. 22, no. 9, pp. 6283–6297, 2023.
- [37] L. Liang, M. Wang, W. Cheng, and W. Zhang, "Double-RIS-assisted orbital angular momentum near-field secure communications," *IEEE Transactions on Wireless Communications*, 2025.
- [38] G. Torcolacci, N. Decarli, and D. Dardari, "Holographic MIMO communications exploiting the orbital angular momentum," *IEEE Open Journal of the Communications Society*, vol. 4, pp. 1452–1469, 2023.
- [39] R. Lyu, et al., "OAM-SWIPT for IoE-driven 6G," *IEEE Communications Magazine*, vol. 60, no. 3, pp. 19–25, 2022.
- [40] M. Jian, et al., "Reconfigurable intelligent surface aided non-coaxial OAM transmission for capacity improvement," in 2022 IEEE/CIC International Conference on Communications in China (ICCC), 2022, pp. 594–599.
- [41] O. A. Saraereh, "Design and performance evaluation of OAM-antennas: A comparative review," *IEEE Access*, vol. 11, pp. 27 992–28 013, 2023.
- [42] J. Xu, K. Bi, R. Zhang, Y. Hao, C. Lan, K. D. McDonald-Maier, X. Zhai, Z. Zhang, and S. Huang, "A small-divergence-angle orbital angular momentum metasurface antenna," *Research*, 2019.
- [43] H. Fukumoto, H. Sasaki, D. Lee, and T. Nakagawa, "Beam divergence reduction using dielectric lens for orbital angular momentum wireless communications," in 2016 International Symposium on Antennas and Propagation (ISAP). IEEE, 2016, pp. 680–681.
- [44] F. Qin, et al., "A high-gain transmitarray for generating dual-mode OAM beams," *IEEE Access*, vol. 6, pp. 61 006–61 013, 2018.
- [45] H. Chung, et al., "Generation of E-band metasurface-based vortex beam with reduced divergence angle," Scientific Reports, vol. 10, no. 1, p. 8289, 2020
- [46] Y. Lin, et al., "Multiple orbital angular momentum circular polarization vortex beam design with equal divergence angle," in 2021 International Conference on Microwave and Millimeter Wave Technology (ICMMT). IEEE, 2021, Conference Proceedings, pp. 1–3.
- [47] L. Liu, et al., "Design of a small-divergence-angle and high-purity OAM metasurface antenna," in 2021 International Conference on Microwave and Millimeter Wave Technology (ICMMT). IEEE, 2021, pp. 1–3.
- [48] G. Junkin, J. ParrÃşn, and A. Tennant, "Characterization of an eightelement circular patch array for helical beam modes," *IEEE Transactions* on Antennas and Propagation, vol. 67, no. 12, pp. 7348–7355, 2019.
- [49] Y. Gong, et al., "Generation and transmission of OAM-carrying vortex beams using circular antenna array," *IEEE Transactions on Antennas and Propagation*, vol. 65, no. 6, pp. 2940–2949, 2017.
- [50] H. Xue, et al., "Model construction, theoretical analysis, and miniaturized implementation of high-order deflected multivortex beams with uniform elliptical array," *IEEE Transactions on Antennas and Propagation*, vol. 70, no. 8, pp. 7234–7239, 2022.
- [51] Y.-M. Zhang and J.-L. Li, "An orbital angular momentum-based array for in-band full-duplex communications," *IEEE antennas and wireless* propagation letters, vol. 18, no. 3, pp. 417–421, 2019.

- **IEEE** Access
- [52] S. Guo, Z. He, and R. Chen, "Generation and numerical simulation of the focused OAM beams," *Engineering Analysis with Boundary Elements*, vol. 135, pp. 359–368, 2022.
- [53] A. Almradi, M. A. B. Abbasi, M. Matthaiou, and V. F. Fusco, "On the spectral efficiency of orbital angular momentum with mode offset," *IEEE Transactions on Vehicular Technology*, vol. 70, no. 11, pp. 11748–11760, 2021.
- [54] D. Liu, et al., "Theoretical analysis and comparison of OAM waves generated by three kinds of antenna array," *Digital Communications and Networks*, vol. 7, no. 1, pp. 16–28, 2021.
- [55] F. Mao, et al., "Massive OAM-MIMO transmission scheme for 5G networks and beyond," IET Communications, vol. 15, no. 7, pp. 973–979, 2021
- [56] X. Hui, et al., "Multiplexed millimeter wave communication with dual orbital angular momentum (OAM) mode antennas," Scientific Reports, vol. 5, no. 1, p. 10148, 2015. [Online]. Available: https://doi.org/10.1038/srep10148
- [57] Z. Zhang, et al., "Experimental demonstration of the capacity gain of plane spiral OAM-based MIMO system," *IEEE Microwave and Wireless Components Letters*, vol. 27, no. 8, pp. 757–759, 2017.
- [58] S. Zheng, et al., "Non-line-of-sight channel performance of plane spiral orbital angular momentum MIMO systems," *IEEE Access*, vol. 5, pp. 25 377–25 384, 2017.
- [59] R. Chen, H. Du, and J. Li, "Indoor communications with OAM array," in 2020 IEEE International Conference on Communications Workshops (ICC Workshops). IEEE, 2020, Conference Proceedings, pp. 1–5.
- [60] F. Mao, et al., "Capacity performance of wireless OAM-based massive MIMO system," Progress In Electromagnetics Research M, vol. 82, pp. 149–156, 2019.
- [61] D. Yang, et al., "Optimizing OAM side-lobe levels using sparse 2D array," in 2019 Photonics & Electromagnetics Research Symposium-Fall (PIERS-Fall). IEEE, 2019, Conference Proceedings, pp. 2199–2206.
- [62] Y. Cho and W. Byun, "Analysis of a uniform rectangular array for generation of arbitrary orbital angular momentum (OAM) modes," *Electronics Letters*, vol. 55, no. 9, pp. 503–504, 2019.
- [63] S. K. Noor, et al., "Generation of OAM waves and analysis of mode purity for 5G sub-6 GHz applications," Comput. Mater. Contin, vol. 74, pp. 2239–2259, 2023.
- [64] A. Z. Golubovic, S. V. Savic, A. Z. Ilic, and M. M. Ilic, "Short-range transmission using OAM-carrying waves generated by uniform circular arrays," *AEU-International Journal of Electronics and Communications*, vol. 165, p. 154643, 2023.
- [65] Q. Bai, A. Tennant, and B. Allen, "Experimental circular phased array for generating OAM radio beams," *Electronics Letters*, vol. 50, no. 20, pp. 1414–1415, 2014. [Online]. Available: https://ietresearch.onlinelibrary.wiley.com/doi/abs/10.1049/el.2014.2860
- [66] B. Qiang, A. Tennant, B. Allen, and M. U. Rehman, "Generation of orbital angular momentum (OAM) radio beams with phased patch array," in 2013 Loughborough Antennas & Propagation Conference (LAPC), 2013, Conference Proceedings, pp. 410–413.
- [67] X. Sun, J. Shao, B. Dan, and Q. Li, "A novel multi-modal OAM vortex electromagnetic wave microstrip array antenna," *Journal of Communica*tions and Information Networks, vol. 4, no. 4, pp. 95–106, 2019.
- [68] X. Y. Liu, et al., "Generation of plane spiral orbital angular momentum waves by microstrip yagi antenna array," *IEEE Access*, vol. 8, pp. 175 688–175 696, 2020.
- [69] D. K. Nguyen, et al., "Antenna gain and link budget for waves carrying orbital angular momentum," Radio Science, vol. 50, no. 11, pp. 1165– 1175, 2015. [Online]. Available: https://agupubs.onlinelibrary.wiley.com/ doi/abs/10.1002/2015RS005772
- [70] M. V. Rao, et al., "Generation of dual-band OAM beam using planar uniform circular array for vehicular communications," Microwave and Optical Technology Letters, vol. 66, no. 1, p. e13717, 2024.
- [71] L. Kang, et al., "A mode-reconfigurable orbital angular momentum antenna with simplified feeding scheme," *IEEE Transactions on antennas and propagation*, vol. 67, no. 7, pp. 4866–4871, 2019.
- [72] D. Yadav, M. D. Upadhayay, and J. Prajapati, "Design constrains in three configurations of UCAs for distortion free orbital angular momentum modes generation," AEU-International Journal of Electronics and Communications, vol. 170, p. 154809, 2023.
- [73] F. Spinello, et al., "Experimental near field OAM-based communication with circular patch array," arXiv preprint arXiv:1507.06889, 2015.

- [74] L. Li and X. Zhou, "Mechanically reconfigurable single-arm spiral antenna array for generation of broadband circularly polarized orbital angular momentum vortex waves," *Scientific Reports*, vol. 8, no. 1, p. 5128, 2018. [Online]. Available: https://doi.org/10.1038/s41598-018-23415-1
- [75] Z.-G. Guo and G.-M. Yang, "Radial uniform circular antenna array for dual-mode OAM communication," *IEEE Antennas and Wireless Propa*gation Letters, vol. 16, pp. 404–407, 2016.
- [76] U. Yesilyurt and H. K. Polat, "Helical circular array configurations for generation of orbital angular momentum beams," *IEEE Antennas and Wireless Propagation Letters*, 2023.
- [77] J. Jiang, et al., "Generation of orbital angular momentum vortex beams with cylindrical and conical conformal array antennas," *International Journal of RF and Microwave Computer-Aided Engineering*, vol. 32, no. 1, p. e22914, 2022.
- [78] D. Weiguo, Z. Yongzhong, Y. Yang, and Z. Kaiwei, "A miniaturized dualorbital-angular-momentum (OAM)-mode helix antenna," *IEEE Access*, vol. 6, pp. 57 056–57 060, 2018.
- [79] C. Deng, et al., "Generation of OAM radio waves using circular vivaldi antenna array," *International Journal of Antennas and Propagation*, vol. 2013, no. 1, p. 847859, 2013.
- [80] S. D. Assimonis, M. A. B. Abbasi, and V. Fusco, "Millimeter-wave multi-mode circular antenna array for uni-cast multi-cast and OAM communication," *Scientific Reports*, vol. 11, no. 1, p. 4928, 2021.
- [81] Y. Yuan, et al., "On the capacity of an orbital angular momentum based MIMO communication system," in 2017 9th International Conference on Wireless Communications and Signal Processing (WCSP), 2017, pp. 1–7.
- [82] X. Ge, R. Zi, X. Xiong, Q. Li, and L. Wang, "Millimeter wave communications with OAM-SM scheme for future mobile networks," *IEEE Journal on Selected Areas in Communications*, vol. 35, no. 9, pp. 2163–2177, 2017.
- [83] Y. Wang, X. Sun, and L. Liu, "A concentric array for generating multi-mode OAM waves," *Journal of Communications and Information Networks*, vol. 7, no. 3, pp. 324–332, 2022.
- [84] C. A. Balanis, Antenna theory: analysis and design. John wiley & sons, 2016.
- [85] T. Yuan, Y. Cheng, H. Wang, and Y. Qin, "Beam steering for electromagnetic vortex imaging using uniform circular arrays," *IEEE Antennas and Wireless Propagation Letters*, vol. 16, pp. 704–707, 2016.
- [86] R. Chen, H. Xu, M. Moretti, and J. Li, "Beam steering for the misalignment in UCA-based OAM communication systems," *IEEE Wireless Communications Letters*, vol. 7, no. 4, pp. 582–585, 2018.
- [87] A. Omar, "Dependence of beamforming on the excitation of orbital angular momentum modes," *IEEE Transactions on Antennas and Propa*gation, vol. 68, no. 10, pp. 7039–7045, 2020.
- [88] K.-R. Liu, S.-H. Wu, L.-L. Yang, and K.-T. Feng, "Hybrid beam focusing for MIMO-OAM communications," in *ICC 2023-IEEE International Conference on Communications*. IEEE, 2023, pp. 5837–5842.
- [89] D. K. Nguyen, et al., "Antenna gain and link budget for waves carrying orbital angular momentum," Radio Science, vol. 50, no. 11, pp. 1165– 1175, 2015.
- [90] M. V. Rao, et al., "Generation of dual-band OAM beam using planar uniform circular array for vehicular communications," Microwave and Optical Technology Letters, vol. 66, no. 1, p. e13717, 2024. [Online]. Available: https://onlinelibrary.wiley.com/doi/abs/10.1002/mop.33717
- [91] K. Liu, et al., "Generation of OAM beams using phased array in the microwave band," *IEEE Transactions on Antennas and Propagation*, vol. 64, no. 9, pp. 3850–3857, 2016.
- [92] Y. Gong, et al., "Generation and transmission of OAM-carrying vortex beams using circular antenna array," *IEEE Transactions on antennas and* propagation, vol. 65, no. 6, pp. 2940–2949, 2017.
- [93] K. Liu, et al., "Orbital-angular-momentum-based electromagnetic vortex imaging," *IEEE Antennas and Wireless Propagation Letters*, vol. 14, pp. 711–714, 2014.
- [94] J. Song, et al., "Design of orbital angular momentum antenna array for generating high-order OAM modes," *Electronics*, vol. 12, no. 24, p. 4891, 2023.
- [95] R. Chen, H. Zhou, W.-X. Long, and M. Moretti, "Spectral and energy efficiency of line-of-sight OAM-MIMO communication systems," *China Communications*, vol. 17, no. 9, pp. 119–127, 2020.
- [96] F. Zheng, S. Ji, and L. Chi, "Selection methods of OAM transceiver arrays in mobile and coaxial scenarios," *IEEE Antennas and Wireless Propagation Letters*, vol. 21, no. 4, pp. 710–714, 2022.

- [97] R. Chen, J. Zhou, W. X. Long, and W. Zhang, "Hybrid circular array and luneberg lens for long-distance OAM wireless communications," *IEEE Transactions on Communications*, vol. 71, no. 1, pp. 485–497, 2023.
- [98] Q. Bai, A. Tennant, E. Cano, and B. Allen, "An experimental phased array for OAM generation," in 2014 Loughborough Antennas and Propagation Conference (LAPC), 2014, Conference Proceedings, pp. 165–168.
- [99] M. V. Rao, et al., "Generation of dual-band OAM beam using planar uniform circular array for vehicular communications," Microwave and Optical Technology Letters, vol. 66, no. 1, p. e13717, 2024. [Online]. Available: https://onlinelibrary.wiley.com/doi/abs/10.1002/mop.33717
- [100] D. Liu, et al., "Design and verification of monopole patch antenna systems to generate orbital angular momentum waves," AIP Advances, vol. 7, no. 9, 2017.
- [101] W. Lee, et al., "Microwave orbital angular momentum mode generation and multiplexing using a waveguide butler matrix," ETRI Journal, vol. 39, no. 3, pp. 336–344, 2017. [Online]. Available: https://onlinelibrary.wiley.com/doi/abs/10.4218/etrij.17.0115.1100
- [102] Y. Yuan, et al., "Capacity analysis of UCA-based OAM multiplexing communication system," in 2015 International Conference on Wireless Communications & Signal Processing (WCSP). IEEE, 2015, pp. 1–5.
- [103] C. Craeye, "On the transmittance between OAM antennas," *IEEE Transactions on Antennas and Propagation*, vol. 64, no. 1, pp. 336–339, 2015.
- [104] A. F. Morabito, L. Di Donato, and T. Isernia, "Orbital angular momentum antennas: Understanding actual possibilities through the aperture antennas theory," *IEEE Antennas and Propagation Magazine*, vol. 60, no. 2, pp. 59–67, 2018.
- [105] H. Li, et al., "A low-profile dual-polarized microstrip antenna array for dual-mode OAM applications," *IEEE Antennas and Wireless Propaga*tion Letters, vol. 16, pp. 3022–3025, 2017.
- [106] Q. y. Shao, H. Xue, and L. Li, "Generation of vortex electromagnetic waves based on helical antenna," in 2019 International Applied Computational Electromagnetics Society Symposium - China (ACES), vol. 1, 2019, pp. 1–2.
- [107] Y. Yang, et al., "Broad-band multiple OAMs" Égeneration with eightarm archimedean spiral antenna (ASA)," IEEE Access, vol. 8, pp. 53 232– 53 239, 2020.
- [108] E. Koohkan, S. Jarchi, A. Ghorbani, and M. Bod, "Orbital angular momentum wave generation/detection based on planar multi-slot-spiral circularly polarized antenna," *Microwave and Optical Technology Letters*, vol. 63, no. 7, pp. 1855–1859, 2021.
- [109] D. Lee, et al., "An experimental demonstration of 28 Ghz band wireless OAM-MIMO (orbital angular momentum multi-input and multi-output) multiplexing," in 2018 IEEE 87th Vehicular Technology Conference (VTC Spring), 2018, Conference Proceedings, pp. 1–5.
- [110] D. Liu, et al., "Multiplexed OAM wave communication with two-OAM-mode antenna systems," IEEE Access, vol. 7, pp. 4160–4166, 2018.
- [111] Q. Feng, Y. Lin, Y. Zheng, and L. Li, "Vortex beam optimization design of concentric uniform circular array antenna with improved array factor," *The Applied Computational Electromagnetics Society Journal (ACES)*, pp. 830–837, 2021.
- [112] A. Habibi Daronkola, et al., "Studying superposition of multiple orbital angular momentum modes for beam concentration using circular arrays for long-range communication," International Journal of RF and Microwave Computer-Aided Engineering, vol. 32, no. 11, p. e23331, 2022.
- [113] S. Guo, Z. He, Z. Fan, and R. Chen, "CUCA based equivalent fractional order OAM mode for electromagnetic vortex imaging," *IEEE Access*, vol. 8, pp. 91070–91075, 2020.
- [114] J. Wu, et al., "Circularly polarized and linear polarized mode multiplexing OAM antenna using sequentially rotated technique," *IEEE Antennas* and Wireless Propagation Letters, vol. 23, no. 4, pp. 1261–1265, 2024.
- [115] S. Zhu, et al., "Low side-lobe high-mode OAM beam generation technique based on concentric ring array," in 2024 IEEE 7th International Conference on Electronic Information and Communication Technology (ICEICT), 2024, pp. 341–343.
- [116] H.-T. Chou, K.-H. Wu, and D.-B. Lin, "Generations of multiple orbital angular momentum modes by 2-D fisheye-lens-based beamformer excited antenna arrays in a spiral configuration," *IEEE Transactions on Antennas and Propagation*, 2023.
- [117] T. Yuan, H. Wang, Y. Qin, and Y. Cheng, "Electromagnetic vortex imaging using uniform concentric circular arrays," *IEEE Antennas and Wireless Propagation Letters*, vol. 15, pp. 1024–1027, 2015.
- [118] A. Z. Ilic, et al., "Performance assessment for OAM antenna arrays," in 2019 IEEE-APS Topical Conference on Antennas and Propagation in

- Wireless Communications (APWC), 2019, Conference Proceedings, pp. 171–173
- [119] A. Ali, "OAM-based electromagnetic metasurfaces for mmwave and THz wireless communications," Thesis, Computer Science and Electronic Engineering, 2023.
- [120] M. Jian, Y. Chen, and G. Yu, "Non-coaxial OAM: Precoding design, misaligned parameter estimation and capacity compensation," *IEEE Access*, vol. 9, pp. 37726–37738, 2021.
- [121] R. Chen, W. X. Long, X. Wang, and L. Jiandong, "Multi-mode OAM radio waves: Generation, angle of arrival estimation and reception with UCAs," *IEEE Transactions on Wireless Communications*, vol. 19, no. 10, pp. 6932–6947, 2020.
- [122] D. Lee, H. Sasaki, Y. Yagi, and H. Shiba, "Orbital angular momentum multiplexing using radio wave and its extension to multishape radio," *Journal of Lightwave Technology*, vol. 41, no. 7, pp. 1985–1996, 2022.
- [123] D. Yadav, M. D. Upadhayay, and J. Prajapati, "Helical array for the generation of OAM wave without phased network," *IEEE Antennas and Wireless Propagation Letters*, 2024.
- [124] R. Chen, M. Zou, X. Wang, and A. Tennant, "Generation and beam steering of arbitrary-order OAM with time-modulated circular arrays," *IEEE Systems Journal*, vol. 15, no. 4, pp. 5313–5320, 2020.
- [125] A. Habibi Daronkola, et al., "Studying superposition of multiple orbital angular momentum modes for beam concentration using circular arrays for long-range communication," International Journal of RF and Microwave Computer-Aided Engineering, vol. 32, no. 11, p. e23331, 2022. [Online]. Available: https://onlinelibrary.wiley.com/ doi/abs/10.1002/mmce.23331
- [126] Q. Wu, X. Jiang, and C. Zhang, "Attenuation of orbital angular momentum beam transmission with a parabolic antenna," *IEEE Antennas and Wireless Propagation Letters*, vol. 20, no. 10, pp. 1849–1853, 2021.
- [127] R. W. Ziolkowski, "The directivity of a compact antenna: An unforgettable figure of merit," EPJ Applied Metamaterials, 2017.
- [128] S. Mishra, R. N. Yadav, and R. P. Singh, "Directivity estimations for short dipole antenna arrays using radial basis function neural networks," *IEEE Antennas and Wireless Propagation Letters*, vol. 14, pp. 1219–1222, 2015.
- [129] R. C. Hansen, Phased Array Antennas. John Wiley & Sons, 2009.
- [130] S. Fu and C. Gao, Optical Vortex Beams: Fundamentals and Techniques. Springer Nature, 2023.
- [131] S. Gao, W. Cheng, H. Zhang, and Z. Li, "High-efficient beam-converging for UCA based radio vortex wireless communications," in 2017 IEEE/CIC International Conference on Communications in China (ICCC). IEEE, 2017, Conference Proceedings, pp. 1–6.
- [132] H. Ma and H. Liu, "Waveform diversity-based generation of convergent beam carrying orbital angular momentum," *IEEE Transactions on Anten*nas and Propagation, vol. 68, no. 7, pp. 5487–5495, 2020.
- [133] J. Chen, "Performance evaluation of electromagnetic OAM waves with circular plate antenna array," in 2019 International Conference on Communications, Information System and Computer Engineering (CISCE). IEEE, 2019, Conference Proceedings, pp. 226–229.
- [134] H. Sasaki, Y. Yagi, H. Fukumoto, and D. Lee, "OAM-MIMO multiplexing transmission system for high-capacity wireless communications on millimeter-wave band," *IEEE Transactions on Wireless Communications*, vol. 23, no. 5, pp. 3990–4003, 2023.
- [135] Y. Ren, et al., "Line-of-sight millimeter-wave communications using orbital angular momentum multiplexing combined with conventional spatial multiplexing," *IEEE Transactions on Wireless Communications*, vol. 16, no. 5, pp. 3151–3161, 2017.
- [136] W. Zhang, et al., "Orbital angular momentum-based communications with partial arc sampling receiving," *IEEE Communications Letters*, vol. 20, no. 7, pp. 1381–1384, 2016.
- [137] A. Alamayreh, N. Qasem, and J. S. Rahhal, "General configuration MIMO system with arbitrary OAM," *Electromagnetics*, vol. 40, no. 5, pp. 343–353, 2020.
- [138] J. A. Stratton, Electromagnetic theory. John Wiley & Sons, 2007, vol. 33.
- [139] Y. Zhang, et al., "Realization of multimode OAM beams with almost the same divergence angles," *International Journal of Antennas* and Propagation, vol. 2021, p. 6683622, 2021. [Online]. Available: https://doi.org/10.1155/2021/6683622
- [140] H. Huang and Z. Zhang, "A single fed wideband mode-reconfigurable OAM metasurface CP antenna array with simple feeding scheme," *International Journal of RF and Microwave Computer-Aided Engineering*, vol. 31, no. 2, p. e22499, 2021.

IEEE*Access*

- [141] H.-F. Huang and S.-N. Li, "High-efficiency planar reflectarray with small-size for OAM generation at microwave range," *IEEE Antennas and Wireless Propagation Letters*, vol. 18, no. 3, pp. 432–436, 2019.
- [142] F. Qin, et al., "A transmission metasurface for generating OAM beams," IEEE Antennas and Wireless Propagation Letters, vol. 17, no. 10, pp. 1793–1796, 2018.
- [143] M. V. Rao, et al., "Series-feed UCA antenna for generating highly azimuthal symmetric OAM beam for unmanned aerial vehicles," AEU - International Journal of Electronics and Communications, vol. 171, p. 154917, 2023. [Online]. Available: https://www.sciencedirect.com/ science/article/pii/S1434841123003916
- [144] J. Yi, et al., "Design and validation of a metasurface lens for converging vortex beams," Applied Physics Express, vol. 12, no. 8, p. 084501, jul 2019. [Online]. Available: https://dx.doi.org/10.7567/1882-0786/ab2c1d
- [145] Y. Li, S. Li, S. W. Wong, and B. Liu, "Analysis of OAM performance using metalenses of different resolutions," *IEEE Access*, vol. 9, pp. 66 982–66 988, 2021.
- [146] D. Liu, W. Wu, L. Gui, and T. Jiang, "OAM mode purity improvement based on antenna array," *Digital Communications and Networks*, 2023. [Online]. Available: https://www.sciencedirect.com/science/article/pii/S2352864823000287
- [147] Y. Yan, et al., "Multipath effects in millimetre-wave wireless communication using orbital angular momentum multiplexing," Scientific reports, vol. 6, no. 1, p. 33482, 2016.
- [148] Z. Zhu, C. Zhang, L. Wang, W. Zheng, and X. Wen, "Research on orbital angular momentum different modes networking method in wireless communication," *IEEE Wireless Communications Letters*, vol. 11, no. 5, pp. 1007–1011, 2022.
- [149] S. Franke-Arnold, B. Jack, J. Leach, and M. J. Padgett, "Angular diffraction," in *Complex Light and Optical Forces III*, vol. 7227. SPIE, 2008, Conference Proceedings, pp. 94–103.
- [150] E. Yao, S. Franke-Arnold, J. Courtial, S. Barnett, and M. Padgett, "Fourier relationship between angular position and optical orbital angular momentum," *Optics Express*, vol. 14, no. 20, pp. 9071–9076, 2006.
- [151] F. Gross, "Smart antennas for wireless communications with MATLAB," McGraw Hills, 2005.
- [152] A. Bole, A. Wall, and A. Norris, "Chapter 1 Basic Radar Principles," in *Radar and ARPA Manual (Third Edition)*, A. Bole, A. Wall, and A. Norris, Eds. Oxford: Butterworth-Heinemann, 2014, pp. 1–28. [Online]. Available: https://www.sciencedirect.com/science/ article/pii/B9780080977522000015
- [153] J. Yang, "Chapter 1 Overview of bistatic SAR," in *Bistatic Synthetic Aperture Radar*, J. Yang, Ed. Elsevier, 2022, pp. 1–76. [Online]. Available: https://www.sciencedirect.com/science/article/pii/B9780128224595000013
- [154] T. Nahar and S. Rawat, "A review of design consideration, challenges and technologies used in 5G antennas," Wireless Personal Communications, vol. 129, no. 3, pp. 1585–1621, 2023.
- [155] S. Zhang, X. Chen, I. Syrytsin, and G. F. Pedersen, "A planar switchable 3-D-coverage phased array antenna and its user effects for 28-Ghz mobile terminal applications," *IEEE Transactions on Antennas and Propagation*, vol. 65, no. 12, pp. 6413–6421, 2017.
- [156] P. Vainikainen, et al., "Recent development of MIMO antennas and their evaluation for small mobile terminals," in MIKON 2008 - 17th International Conference on Microwaves, Radar and Wireless Communications, 2008, Conference Proceedings, pp. 1–10.
- [157] Y. Diao, M. Su, Y. Liu, S. Li, and W. Wang, "Compact and multiband dielectric resonator antenna for mobile terminals," in 2015 IEEE International Symposium on Antennas and Propagation & USNC/URSI National Radio Science Meeting, 2015, Conference Proceedings, pp. 1724–1725.
- [158] J. Xu, et al., "Recent progress on RF orbital angular momentum antennas," Journal of Electromagnetic Waves and Applications, vol. 34, no. 3, pp. 275–300, 2020.
- [159] T. Zhengjuan, C. Rui, L. Wenxuan, Z. Hong, and M. Marco, "Broad-band beam steering for misaligned multi-mode OAM communication systems," *Journal of Systems Engineering and Electronics*, vol. 32, no. 4, pp. 779–788, 2021.
- [160] M. Veysi, C. Guclu, F. Capolino, and Y. Rahmat-Samii, "Revisiting orbital angular momentum beams: Fundamentals, reflectarray generation, and novel antenna applications," *IEEE Antennas and Propagation Mag*azine, vol. 60, no. 2, pp. 68–81, 2018.
- [161] M. Jofre, et al., "Magnetoelectric dipole antenna framework supporting orbital angular momentum modes," *IEEE Transactions on Antennas and Propagation*, vol. 72, no. 4, pp. 3064–3072, 2024.

[162] Y. Zhao, et al., "Advanced artificial doppler shift manipulation with rotational vortex beams in space-time digital-coding RIS system: A practical approach," in 2024 IEEE VTS Asia Pacific Wireless Communications Symposium (APWCS), 2024, pp. 1–5.



ZIHAO WANG has been studying with the University of Southampton to pursue his Ph.D. degree since 2022. His current research focuses mainly on the applications of orbital angular momentum (OAM) in wireless communications, in particular, in millimeter wave (mmWave) and terahertz (THz) communications.



MOHAMMED EL-HAJJAR (M'02, SM'14) is a Professor of Signal Processing for Wireless Communications in the School of Electronics and Computer Science in the University of Southampton. He is the recipient of several academic awards and has published a Wiley-IEEE book and more than 100 IEEE journal and conference papers and in excess of 10 patents. MohammedâĂŹs research interests include the design of intelligent and energy-efficient transceivers, MIMOs, millimeter wave

communications, and machine learning for wireless communications. Mohammed's research is funded by the Engineering and Physical Sciences Research Council, the Royal Academy of Engineering and many industrial partners.



LIE-LIANG YANG (M'98, SM'02, F'16) is the professor of Wireless Communications in the School of Electronics and Computer Science at the University of Southampton, UK. He received his MEng and PhD degrees in communications and electronics from Northern (Beijing) Jiaotong University, Beijing, China in 1991 and 1997, respectively, and his BEng degree in communications engineering from Shanghai TieDao University, Shanghai, China in 1988. He has research

interest in wireless communications, wireless networks and signal processing for wireless communications, as well as molecular communications and nano-networks. He has published 500+ research papers in journals and conference proceedings, authored/co-authored 4 books and 10+ chapters. More information about his research publications can be found at https://www.ecs.soton.ac.uk/people/llyang. He is a fellow of the IEEE, IET, AAIA and AIIA, and was a distinguished lecturer of the IEEE VTS. He has served various roles for some research journals, and acted different roles for organization of conferences.

0 0 0